Vol. 000, 1–24 (2022) Preprint 8 July 2022 Compiled using MNRAS LaTeX style file v3.0

The statistical theory of dark matter flow and high order kinematic and dynamic relations for velocity and density correlations

Zhijie (Jay) Xu,[1★]
[1] *Physical and Computational Sciences Directorate, Pacific Northwest National Laboratory; Richland, WA 99352, USA*

Accepted XXX. Received YYY; in original form ZZZ

ABSTRACT
Statistical theory for self-gravitating collisionless dark matter flow is not fully developed because of 1) intrinsic complexity involving constant divergence flow on small scale and irrotational flow on large scale; 2) lack of self-closed description for peculiar velocity; and 3) mathematically challenging. To better understand dark matter flow, kinematic and dynamic relations among different statistical measures of velocity must be developed for different types of flow. In this paper, a compact derivation is presented to formulate general kinematic relations on any order for incompressible, constant divergence, and irrotational flow. Results are validated by N-body simulation. Dynamic relations can only be determined from self-closed description of velocity evolution. On large scale, we found i) third order velocity correlation can be related to density correlation or pairwise velocity; ii) effective viscosity in adhesion model originates from velocity fluctuations; iii) negative viscosity is due to inverse energy cascade; iv) qth order velocity correlations follow $\propto a^{(q+2)/2}$ for odd q and $\propto a^{q/2}$ for even q; v) overdensity is proportional to density correlation on the same scale, $\langle\delta\rangle \propto \langle\delta\delta'\rangle$; vi) (reduced) velocity dispersion is proportional to density correlation on the same scale. On small scale, self-closed description for velocity evolution is developed by decomposing velocity into motion in halo and motion of halos. Vorticity, enstrophy, and energy evolution can all be derived from self-closed equation for velocity. Dynamic relation is derived to relate second and third order correlations. Third moment of pairwise velocity is determined by energy cascade rate ϵ_u or $\langle(\Delta u_L)^3\rangle \propto \epsilon_u ar$. Finally, combined kinematic and dynamic relations determines the exponential and one-fourth power law velocity correlations on large and small scales, respectively.

Key words: Dark matter; N-body simulations; Theoretical models; Velocity correlations

CONTENTS

★ E-mail: zhijie.xu@pnnl.gov; zhijiexu@hotmail.com

1 INTRODUCTION

The statistics of cosmic velocity field is valuable to probe large scale structure formation and density fluctuation and constrain cosmology parameters (Ma et al. 2015). The statistical analysis is mostly applied to the pairwise velocity, i.e. the velocity difference of a mass pair along the direction of their separation or the difference between two longitudinal velocities (Xu 2022f). The pairwise velocity was originally introduced to describe the dynamic evolution of a system of self-gravitating particles (Davis & Peebles 1977) and was later applied to probe the cosmological density parameter (Ferreira et al. 1999; Juszkiewicz et al. 2000). The lower-order moments of pairwise velocity was also proposed as a diagnostic tool for laws of gravity on large scale (Hellwing et al. 2014). Another common statistical measure is the two-point second order velocity correlation functions that was introduced in 1980s to quantify the cosmic velocity field (Gorski 1988). It was later applied to real dataset of local Superclusters samples (Gorski et al. 1989) and SFI catalog of peculiar velocities (Borgani et al. 2000).

Directly measuring velocity correlations from real samples is still very challenging in practice since only the radial velocity component can be directly observed. On the other side, N-body simulation is an invaluable tool to study the dynamics of collisionless dark matter flow on different scales, capture the very complex gravitational collapse and many other effects beyond standard Newtonian approximations (Angulo et al. 2012; Springel 2005; Peebles et al. 1989; Efstathiou et al. 1985). The peculiar velocity from N-body simulations is relatively accessible with large amount of simulation data available. In addition, tremendous amount of knowledge on the nature of self-gravitating collisionless dark matter flow (SG-CFD) can be obtained from this practice. Some results for second order statistics were already discussed previously (Xu 2022f) and this paper will generalize these results to high order statistics.

Traditionally, two approaches can be applied to study the velocity field in N-body system. The first one is a halo-based approach. All particles in entire system are divided into particles in halos and out-of-halo particles. The density, velocity, and acceleration distributions of halo and out-of-halo particles evolve in different ways, which can be studied separately (Xu 2022h,j). Our previous study primarily falls into this category, of which the inverse mass and energy cascade and halo mass functions can be rigorously developed (Xu 2021a,b,f, 2022g). The maximum entropy distributions of dark matter particle velocity and energy were also formulated (Xu 2021c,e). Relevant applications of mass/energy cascade theory in dark matter flow are also presented for dark matter particle mass and properties (Xu 2022i), MOND (modified Newtonian dynamics) theory (Xu 2022j), and baryonic-to-halo mass relation (Xu 2022k).

A different alternative strategy (correlation-based approach) of statistical analysis works with statistical measures of velocity field. The correlation, structure, dispersion, and spectrum functions are among the most important statistical measures to quantify the peculiar velocity field (Xu 2022f). In this approach, the scale and redshift variation of these statistical measures can be studied in detail (Xu 2022h; Kitaura et al. 2016; Pueblas & Scoccimarro 2009). Halo structure is not explicitly involved in this approach. However, on small scale, most pairs of particles are from the same halo. While on large scale, pairs of particles are from different halos. Therefore, effect of halo structure on statistics can be clearly identified through the scale dependence of these statistical measures. Statistical analysis by projecting velocity field onto structured grids may involve information loss. In this paper, we directly compute statistical measures of different order that contain the most complete information of a N-body system at different scales and redshifts.

In principle, both halo-based and correlation-based approaches have their own strength and weakness, while in this paper we primarily focus on the correlation-based statistical analysis of velocity field that was originally developed in the theory of incompressible homogeneous turbulence (Batchelor 1953). The velocity correlation functions, firstly introduced by Taylor in 1930s (Taylor 1935, 1932), play a central role in the statistical theory of turbulence. Other statistical measures are related to correlation functions and describing how energy and enstrophy are distributed on different scales.

The statistical theory of stochastic flow is mostly concerned about two types of relations: i) the kinematic relations between statistical measures of the same order; and ii) the dynamic relations between statistical measures of different orders. The kinematic relations can be developed for a given nature of flow (incompressible, constant divergence, or irrotational) under the assumption of translational and rotational symmetry. However, the dynamic relations can only be developed from self-closed dynamic equations for evolution of velocity field, such as the Burgers' or Navier-Stokes equation. In fact, the celebrated Kolmogorov's four-fifth law is an exact result of the dynamic relations derived from Navier-Stokes equation (de Karman & Howarth 1938; Kolmogoroff 1941a,b).

By contrast, the statistical theory for self-gravitating collisionless dark matter flow (SG-CFD) is not completely developed and far from satisfactory due to several reasons:

(i) SG-CFD flow is intrinsically much more complex with different nature of flow on different scales, i.e. a constant divergence flow on small scale and an irrotational flow on large scale (Xu 2022f). The kinematic and dynamic relations need to be developed separately for both types of flow on different scales.
(ii) Dynamic equations of velocity (Jeans' equation) on small scale are not self-closed. No dynamic relations can be derived without a self-closed dynamics for velocity evolution.
(iii) Existing work mostly focus on the first and second order velocity statistics, while the peculiar velocity field contains much richer information beyond the second order. One example is the third order velocity correlations that is intimately related to the energy cascade and transfer across sales (Eqs. (128) and (192)). However, it is very challenging to explore high order statistics, as that inherently involves tensors and vector calculus of great complexity.

The primary purpose of this paper is to establish the formal language of statistical theory for collisionless dark matter flow by introducing basic notations, putting in place necessary equations, and laying down the fundamental rules. The theory itself is intrinsically complex due to stochasticity, nonlinearity, and multiscale nature, while we are still able to appreciate the beauty of nature as evidenced by the hidden symmetry in kinematic and dynamic relations. From this practice, we are able to demonstrate that on large scale,

(i) The third order correlation determines the rate of energy cascade;
(ii) The effective viscosity originates from velocity fluctuations and negative viscosity $\nu(a)$ reflects the inverse energy cascade;
(iii) The qth order correlation functions scale as $\propto a^{(q+2)/2}$ for odd order q and scale as $\propto a^{q/2}$ for even order q;
(iv) Mean overdensity on a given scale r is proportional to the density correlation on the same scale, i.e. $f(\Omega_m)\langle\delta\rangle \approx \langle\delta\delta'\rangle$. The existence of low density void region can be related to the negative density correlation $\langle\delta\delta'\rangle < 0$ on that scale;
(v) (Reduced) velocity dispersion on a given scale is proportional to the density correlation on the same scale, i.e. $\langle u^2\rangle/(3u^2) - 1 \propto \langle\delta\delta'\rangle$. Low density void region has relatively small velocity dispersion;
(vi) The exponential velocity correlation originates from a combined kinematic and dynamic relations on large scale;

While on small scale, a self-closed description for velocity evolution is developed along with the associated dynamic relations. The third order correlation and structure functions on small scale can be directly related to the constant rate of energy cascade ε_u.

There is tremendous amount of knowledge that can be learned from this practice, much more than what we can present here. With the second order statistics presented in (Xu 2022f), this paper is organized as follows: Section 2 introduces the N-body simulation data used, followed by the third order statistical measures in Section 3. The general kinematic relations are presented in Section 4 with results from N-body simulations for comparison and validation in Section 5. Finally, the dynamic relations are formulated on large and small scales in Sections 6 and 7, respectively.

2 N-BODY SIMULATIONS AND NUMERICAL DATA

The numerical data are public available and generated from N-body simulations carried out by the Virgo consortium. A comprehensive description of the data can be found in (Frenk et al. 2000; Jenkins et al. 1998). As the first step, current study uses simulation runs with $\Omega = 1$ and the standard CDM power spectrum (SCDM) to focus on the matter-dominant gravitational flow. Similar analysis can be extended to other model with different assumptions and parameters in the future. Current simulation includes 17 million particles with

Table 1. Numerical parameters of N-body simulation

Run	Ω_0	Λ	h	Γ	σ_8	L (Mpc/h)	N	m_p $M_\odot/h$	l_{soft} (Kpc/h)
SCDM1	1.0	0.0	0.5	0.5	0.51	239.5	256^3	2.27×10^{11}	36

particle mass of $2.27\times10^{11}\ M_\odot/h$. The simulation box sizes around 240 Mpc/h, where h is the reduced Hubble constant. The same set of data has been widely used in a number of studies from clustering statistics (Jenkins et al. 1998) to formation of cluster halos in large scale environment (Colberg et al. 1999), and test of models for halo abundances and mass functions (Sheth et al. 2001). Some key numerical parameters of N-body simulation are listed in Table 1.

Two relevant datasets from this N-boby simulation, i.e. halo-based and correlation-based statistics of dark matter flow, can be found at Zenodo.org (Xu 2022a,b), along with the accompanying presentation slides, "A comparative study of dark matter flow & hydrodynamic turbulence and its applications" (Xu 2022c). All data files are also available on GitHub (Xu 2022d).

3 THIRD AND HIGH ORDER VELOCITY STATISTICS

The real-space two-point second order statistical measures have been introduced for density, velocity, and potential fields along with the kinematic relations developed for different types of flow (Xu 2022f). In this section, two-point third order statistical measures are introduced along with the kinematic relations. The SG-CFD flow is of constant divergence on small scale and irrotational on large scale. The constant divergence flow and incompressible flow share the same kinematic relations for even order statistical measures, while they can be different for odd order statistics (Xu 2022f). Same as previous discussion for second order statistics, we restrict our discussion to homogeneous and isotropic flow that will significantly simplify velocity correlation tensors and the development of theory. Third order statistical measures for a specific type of flow, i.e. incompressible, constant divergence, or irrotational flow, are all discussed in detail.

3.1 Third order velocity correlation tensor

Due to homogeneous and isotropic symmetry, the two-point third order velocity correlation tensor can be generally defined as

$$\begin{aligned} Q_{ijk}(\mathbf{x},\mathbf{r}) &= Q_{ijk}(\mathbf{r}) = Q_{ijk}(r) \\ &= \left\langle u_i(\mathbf{x})\,u_j(\mathbf{x})\,u_k\left(\mathbf{x}'\right)\right\rangle = \left\langle u_i u_j u_k'\right\rangle \end{aligned} \tag{1}$$

for velocity field $\mathbf{u}$ at two different locations separated by a distance r, where $\mathbf{x}' = \mathbf{x}+\mathbf{r}$ (Fig. 1). The prime notation indicates the field evaluated at location $\mathbf{x}'$, with u_L and u_T standing for the longitudinal and transverse velocities in Fig. 1.

For third order isotropic tensor $Q_{ijk}(r)$, symmetry requires

$$Q_{ijk}(-r) = \left\langle u_i' u_j' u_k\right\rangle = -\left\langle u_i u_j u_k'\right\rangle = -Q_{ijk}(r). \tag{2}$$

The most general form of the isotropic third order correlation tensor can be written as,

$$\begin{aligned} Q_{ijk}(r) &= A_3(r)\,r_i r_j r_k + B_3(r)\,r_i\delta_{jk} \\ &\quad + C_3(r)\,r_j\delta_{ki} + D_3(r)\,r_k\delta_{ij}, \end{aligned} \tag{3}$$

where $A_3(r)$, $B_3(r)$, $C_3(r)$ and $D_3(r)$ are all symmetric regular functions of scale r. Because of the symmetry about indexes i and j (using definition in (1)),

$$Q_{ijk}(r) = Q_{jik}(r) \quad \text{leads to} \quad B(r) = C(r). \tag{4}$$

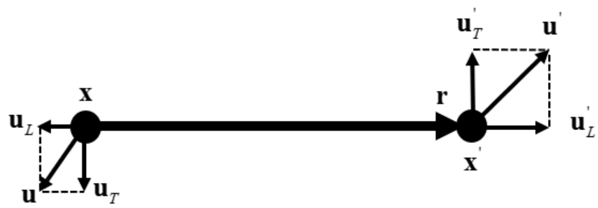

Figure 1. A schematic plot for the longitudinal (u_L and u_L') and transverse (u_T and u_T') velocities for a particle pair separated by a distance of r.

The final form of third order correlation tensor simply reads

$$Q_{ijk}(r) = A_3(r)\,r_i r_j r_k + B_3(r)\left(r_i\delta_{jk} + r_j\delta_{ki}\right) + D_3(r)\,r_k\delta_{ij}, \tag{5}$$

which is fully determined by three scalar functions A_3, B_3 and D_3.

Using contraction in index, the longitudinal triple (third order) correlation function is defined as

$$L_3(r) = Q_{ijk}\hat{r}_i\hat{r}_j\hat{r}_k = \left\langle u_L^2 u_L'\right\rangle = A_3 r^3 + (2B_3 + D_3)\,r, \tag{6}$$

where $\hat{r}_i = r_i/r$ is the normalized Cartesian components of vector $\boldsymbol{r}$ satisfying $\hat{r}_i\hat{r}_i = 1$. Einstein summation is employed. Here $u_L = \mathbf{u}\cdot\mathbf{r} = u_i r_i$ is the longitudinal velocity in Fig. 1. Two total third order correlation functions can be defined as,

$$\begin{aligned} R_3(r) &= \frac{1}{2}Q_{ijk}\left(\delta_{ik}\hat{r}_j + \delta_{jk}\hat{r}_i\right) \\ &= \left\langle u_L \mathbf{u}\cdot\mathbf{u}'\right\rangle = A_3 r^3 + (4B_3 + D_3)\,r, \end{aligned} \tag{7}$$

$$R_{31}(r) = Q_{ijk}\delta_{ij}\hat{r}_k = \left\langle \mathbf{u}\cdot\mathbf{u}u_L'\right\rangle = A_3 r^3 + (2B_3 + 3D_3)\,r. \tag{8}$$

The transverse third-order correlation function can be defined as,

$$T_3(r) = \left\langle u_L \mathbf{u}_T\cdot\mathbf{u}_T'\right\rangle/2 = (R_3 - L_3)/2 = B_3 r, \tag{9}$$

with transverse velocity perpendicular to vector $\boldsymbol{r}$ (Fig. 1),

$$\mathbf{u}_T = -(\mathbf{u}\times\mathbf{r}\times\mathbf{r}) = \mathbf{u} - (\mathbf{u}\cdot\mathbf{r})\,\mathbf{r}. \tag{10}$$

All third order correlation functions satisfy the odd symmetry $f(-r) = -f(r)$.

Next, the divergence and curl of third-order correlation tensor are formulated. Some tensor/vector algebra are involved and only the final results are presented here for later use. The divergence reads

$$\begin{aligned} Q_{ijk,k} &= \frac{\partial Q_{ijk}(r)}{\partial r_k} = \frac{\partial\left\langle u_i u_j u_k'\right\rangle}{\partial r_k} \\ &= \left(5A_3 + \frac{\partial A_3}{\partial r}r + \frac{2}{r}\frac{\partial B_3}{\partial r}\right)r_i r_j + \left(2B_3 + \frac{\partial D_3}{\partial r}r + 3D_3\right)\delta_{ij}, \\ Q_{iik,k} &= Q_{ijk,k}\delta_{ij} \\ &= \left(5A_3 + \frac{\partial A_3}{\partial r}r + \frac{2}{r}\frac{\partial B_3}{\partial r}\right)r^2 + 3\left(2B_3 + \frac{\partial D_3}{\partial r}r + 3D_3\right), \end{aligned} \tag{11}$$

and

$$\begin{aligned} Q_{ijk,i} &= \frac{\partial Q_{ijk}(r)}{\partial r_i} = \left(5A_3 + \frac{\partial A_3}{\partial r}r + \frac{1}{r}\frac{\partial B_3}{\partial r} + \frac{1}{r}\frac{\partial D_3}{\partial r}\right)r_j r_k \\ &\quad + \left(4B_3 + \frac{\partial B_3}{\partial r}r + D_3\right)\delta_{jk}. \end{aligned} \tag{12}$$

Other derivatives can be derived from Eq. (12),

$$Q_{ijk,ij} = \frac{\partial Q_{ijk}(r)}{\partial r_i \partial r_j} = \left(r^2\frac{\partial^2 A_3}{\partial r^2} + 10r\frac{\partial A_3}{\partial r} + 20A_3 + 2\frac{\partial^2 B_3}{\partial r^2} + \frac{8}{r}\frac{\partial B_3}{\partial r} + \frac{\partial^2 D_3}{\partial r^2} + \frac{4}{r}\frac{\partial D_3}{\partial r}\right) r_k, \tag{13}$$

$$Q_{iki,k} = Q_{ikk,i} = Q_{ijk,i}\delta_{jk} = 5A_3 r^2 + \frac{\partial A_3}{\partial r}r^3 + 12B_3 + 4r\frac{\partial B_3}{\partial r} + 3D_3 + r\frac{\partial D_3}{\partial r}, \tag{14}$$

where symmetry condition (Eq. (4)) is used for deriving Eq. (14). With definition of correlation functions R_3 and R_{31} in Eqs. (7) and (8), Eqs. (11) and (14) can be concisely written as

$$Q_{iki,k} = Q_{ijk,i}\delta_{jk} = Q_{ikk,i} = \frac{1}{r^2}\left(r^2 R_3\right)_{,r}$$

and (15)

$$Q_{iik,k} = \frac{1}{r^2}\left(r^2 R_{31}\right)_{,r}.$$

Similarly, the curl of third order velocity correlation tensor reads

$$\nabla \times Q_{mni}(r) = \varepsilon_{ijk} Q_{mnk,j} = \left(A_3 - \frac{1}{r}\frac{\partial B_3}{\partial r}\right)\left(\varepsilon_{imk} r_n r_k + \varepsilon_{ink} r_m r_k\right). \tag{16}$$

where ε_{ijk} is the standard Levi-Civita symbol.

3.1.1 *Kinematic relations for incompressible flow*

This section formulates the kinematic relations for incompressible flow following the classical approach in the theory of turbulence. A new and more compact formulation is presented in Appendix A that facilitates the generalization to arbitrary order. First, the divergence free requirement in Eq. (11) leads to two separate relations

$$5A_3 r + \frac{\partial A_3}{\partial r}r^2 + 2\frac{\partial B_3}{\partial r} = 0, \tag{17}$$

$$2B_3 + \frac{\partial D_3}{\partial r}r + 3D_3 = 0. \tag{18}$$

Differentiating Eq. (18) and subtracting Eq. (17) leads to

$$\left(\frac{\partial D_3}{\partial r}r\right)_{,r} + 3\frac{\partial D_3}{\partial r} = r^2\frac{\partial A_3}{\partial r} + 5A_3 r = \left(A_3 r^2\right)_{,r} + 3A_3 r. \tag{19}$$

From Eqs.(18) and (19)), we should have

$$A_3 = \frac{1}{r}\frac{\partial D_3}{\partial r} \quad \text{and} \quad A_3 r^2 + 2B_3 + 3D_3 = 0. \tag{20}$$

Equation (18) can be analytically solved (using Eqs. (6) and (20)),

$$B_3 = -\frac{r}{2}\frac{\partial D_3}{\partial r} - \frac{3}{2}D_3 \quad \text{and} \quad D_3 = -L_3/(2r). \tag{21}$$

With all scalar functions A_3 ,B_3, and D_3 expressed in terms of the longitudinal correlation $L_3(r)$, the third order correlation tensor can be expressed as (prime denotes the derivative with respect to r)

$$Q_{ijk}(r) = \frac{L_3 - rL_3'}{2}\hat{r}_i\hat{r}_j\hat{r}_k + \frac{2L_3 + rL_3'}{4}\left(\hat{r}_i\delta_{jk} + \hat{r}_j\delta_{ki}\right) - \frac{L_3}{2}\hat{r}_k\delta_{ij}. \tag{22}$$

From Eqs. (13), (17) and (18), we have $Q_{ijk,ij} = 0$. Since the first order isotropic tensor for incompressible flow must be zero (see Xu 2022f, Section 3.1), we should have

$$Q_{ijk,ij} = Q_{ijk,ik} = Q_{ijk,jk} = 0. \tag{23}$$

Multiplying Eq. (22) by δ_{jk} and taking the divergence,

$$Q_{iki,k} = Q_{ijk,i}\delta_{jk} = Q_{ikk,i} = \frac{1}{r^2}\left(R_3 r^2\right)_{,r} = \frac{1}{2r^2}\frac{\partial}{\partial r}\left(\frac{1}{r}\frac{\partial}{\partial r}\left(r^4 L_3\right)\right), \tag{24}$$

with the following identity used

$$\left(\hat{r}_i\right)_{,j} = \frac{1}{r}\left(\delta_{ij} - \hat{r}_i\hat{r}_j\right) = \left(\hat{r}_j\right)_{,i} \quad \text{and} \quad \left(\hat{r}_i\right)_{,i} = \frac{2}{r}. \tag{25}$$

The kinematic relations between third-order correlations can be easily obtained by contraction in index notation from Eq. (22) (using definitions (7) and (9)) such that

$$R_3 = \frac{1}{2r^3}\left(r^4 L_3\right)_{,r}, T_3 = \frac{1}{4r}\left(r^2 L_3\right)_{,r},$$

and (26)

$$r^2\left(r^2 R_3\right)_{,r} = 2\left(r^4 T_3\right)_{,r}.$$

These kinematic relations will be generalized to higher order in Section 4 with a new method of derivation. From Eqs. (20) and (8), the total correlation function R_{31} vanishes for incompressible flow,

$$R_{31}(r) = \left\langle \mathbf{u}\cdot\mathbf{u}u_L'\right\rangle = 0. \tag{27}$$

The same correlation R_{31} does not vanish for dark matter flow, i.e. two types of flow are different in odd order correlations (Fig. 8).

3.1.2 *Kinematic relations for constant divergence on small scale*

The kinematic relations for constant divergence flow are different from incompressible flow for odd order correlations. The peculiar radial flow u_r in virialized halos satisfies $\mathbf{u_r} = -Ha\mathbf{r}$ from stable clustering hypothesis (Xu 2021d). The divergence of peculiar velocity $\nabla\cdot\mathbf{u} = -3Ha$ (in local spherical coordinate), i.e. a spatially constant divergence (see Xu 2022e, Eq.(60)). Without loss of generality, let's assume $\nabla\cdot\mathbf{u} = \theta(t)$, where θ is a constant in space. The divergence of third order correlation tensor simply reads

$$Q_{ijk,k} = \nabla'\cdot\left\langle u_i(\mathbf{x})\,u_j(\mathbf{x})\,u_k\left(\mathbf{x}'\right)\right\rangle = \left\langle u_i(\mathbf{x})\,u_j(\mathbf{x})\frac{\partial u_k\left(\mathbf{x}'\right)}{\partial x_k'}\right\rangle = \theta\left\langle u_i u_j\right\rangle, \tag{28}$$

where the prime stands for taking derivative at location $\mathbf{x}'$. The constant divergence requires (Eq. (11)),

$$Q_{ijk,k} = \left\langle u_i u_j\right\rangle\theta = \left(5A_3 + \frac{\partial A_3}{\partial r}r + \frac{2}{r}\frac{\partial B_3}{\partial r}\right)r_i r_j + \left(2B_3 + \frac{\partial D_3}{\partial r}r + 3D_3\right)\delta_{ij}. \tag{29}$$

Multiplying $\hat{r}_i\hat{r}_j$ on both sides of Eq. (29) gives

$$\left\langle u_L^2\right\rangle\theta = \left(5A_3 + \frac{\partial A_3}{\partial r}r + \frac{2}{r}\frac{\partial B_3}{\partial r}\right)r^2 + \left(2B_3 + \frac{\partial D_3}{\partial r}r + 3D_3\right). \tag{30}$$

Using definitions of correlation functions in Eqs. (6) and (7), an exact kinematic relation can be obtained between correlation functions, longitudinal dispersion $\langle u_L^2\rangle$ and divergence θ,

$$R_3 + \frac{1}{2}\left\langle u_L^2\right\rangle\theta r = \frac{1}{2r^3}\left(r^4 L_3\right)_{,r} \tag{31}$$

Similarly, multiplying δ_{ij} on both sides of Eq. (29) leads to

$$\left\langle u^2\right\rangle\theta=\left(5A_3+\frac{\partial A_3}{\partial r}r+\frac{2}{r}\frac{\partial B_3}{\partial r}\right)r^2+3\frac{\partial D_3}{\partial r}r+6B_3+9D_3. \quad (32)$$

An exact relation for R_{31} and total velocity dispersion $\langle u^2\rangle$ on scale r can be obtained from Eqs. (11) and (15),

$$\left\langle u^2\right\rangle\theta=\frac{1}{r^2}\left(r^2R_{31}\right)_{,r}. \quad (33)$$

With $\langle u^2\rangle\approx 3\langle u_L^2\rangle$ (see Xu 2022h, Fig. 20) that is exact on both small and large scales, the kinematic relation between three third order correlation functions finally reads,

$$R_3+\frac{1}{6r}\left(r^2R_{31}\right)_{,r}=\frac{1}{2r^3}\left(r^4L_3\right)_{,r}. \quad (34)$$

For small r with velocity dispersion $\langle u_L^2\rangle$ independent of r , solution of R_{31} from Eq. (33) is

$$R_{31}=\theta\left\langle u_L^2\right\rangle r. \quad (35)$$

In particular, with $\theta=0$, kinematic relations Eqs. (31), (33), and (34) reduce to Eqs. (26) and (27) for incompressible flow, as expected.

3.1.3 Kinematic relations for irrotational flow on large scale

Dark matter flow is irrotational on large scale. The curl free condition from Eq. (16) leads to the following requirement on large scale,

$$\frac{1}{r}\frac{\partial B_3}{\partial r}=A_3. \quad (36)$$

The kinematic relations between velocity correlations can be similarly found from Eqs. (6)-(9),

$$(rR_3)_{,r}+R_{31}=\frac{1}{r^3}\left(r^4L_3\right)_{,r},\quad 3R_3-R_{31}=\frac{2}{r^3}\left(r^4T_3\right)_{,r},$$

and

$$3L_3-R_{31}=2\left(rT_3\right)_{,r}. \quad (37)$$

All kinematic relations developed for constant divergence flow on small scale and irrotational flow on large scale can be validated by N-body simulations and presented in Section 5.

3.2 Third and higher order velocity structure functions

Structure functions are statistical measures to describe how the system energy is distributed and transferred across scales. Third order longitudinal velocity structure function is defined as

$$S_3^{lp}(r)=\left\langle(\Delta u_L)^3\right\rangle=\left\langle\left(u_L'-u_L\right)^3\right\rangle=6L_3(r)-2\left\langle u_L^3\right\rangle, \quad (38)$$

where Δu_L is the pairwise velocity. More generally, the mth order longitudinal structure function can be defined as

$$S_m^{lp}=\left\langle(\Delta u_L)^m\right\rangle=\left\langle\left(u_L'-u_L\right)^m\right\rangle. \quad (39)$$

Models for structure functions are presented for self-gravitating collisionless dark matter flow. On small scale, the reduced even order structure functions follow a two-third law (see Xu 2022h, Eq. (56) and Fig. 22). With pre-factor determined by the rate of energy production ε_u from inverse energy cascade (Xu 2021f), we have

$$S_{2n}^{lp}(r)-S_{2n}^{lp}(0)\propto(-\varepsilon_u)^{2/3}r^{2/3}, \quad (40)$$

where $S_{2n}^{lp}(0)$ is the (2n)th moment of limiting distribution of pairwise velocity $\Delta u_L$when $r\to 0$ (see Xu 2022h, Eq. (61) and Table 4). Here $\varepsilon_u<0$ reflects the inverse mass cascade with

$$-\varepsilon_u=\frac{3}{2}\frac{u_0^2}{t_0}=\frac{9}{4}u_0^2H_0\approx 0.6345\frac{u_0^3}{Mpc/h}, \quad (41)$$

where t_0 and H_0 are the present time and Hubble constant, u_0 is the one-dimensional velocity dispersion at present epoch.

On small scale, the odd order structure functions are predicted as

$$S_{2n+1}^{lp}(r)=(2n+1)\,S_1^{lp}(r)\,S_{2n}^{lp}(r) \quad (42)$$

from generalized stable clustering hypothesis (GSCH). This is based on a two-body collapse model (see TBCM model Xu 2021d, Eq. (123)). With $S_1^{lp}(r)=-Har$ (see Xu 2021d, Eq. (117)),

$$\begin{aligned}S_{2n+1}^{lp}(r)&=-(2n+1)\,HarS_{2n}^{lp}(0)\\&=-2^n(2n+1)\,K_{2n}(\Delta u_L,0)\,Haru^{2n},\end{aligned} \quad (43)$$

where $K_{2n}(\Delta u_L,0)$ is the generalized kurtosis of the distribution of pairwise velocity $\Delta u_L$when $r\to 0$ (see Xu 2022h, Table 4).

4 KINEMATIC RELATIONS FOR VELOCITY CORRELATIONS OF ARBITRARY ORDER

In this section, we formulate general kinematic relations of any order (beyond second and third order) for different types of flow. This is a very challenging task involving significant amount of tensor/vector algebra and calculus. Readers can simply skip details of derivation in Appendix A and directly jump to final results, i.e. Eqs. (53)-(55) for incompressible flow, Eq. (62) for constant divergence on small scale, and Eqs. (63)-(65) for irrotational flow on large scale.

4.1 General correlation functions on any order

The two-point velocity correlation tensor Q of arbitrary order p can be defined as,

$$\left({}_{(p)}Q_{ijk..mn}\right)=\left\langle u_iu_ju_k...u_mu_n'\right\rangle. \quad (44)$$

Scalar correlation functions are defined by tensor contraction of Q (similar to Eqs. (6), (7), and (8)). For even number q, the total correlation functions of order $(p,q+1)$ is defined as

$$R_{(p,q+1)}=\left\langle u^qu_L^{p-q-2}u_iu_i'\right\rangle=\left\langle u^qu_L^{p-q-2}\mathbf{u}\cdot\mathbf{u}'\right\rangle. \quad (45)$$

For even number q, the longitudinal and transverse correlation functions of order (p,q) are defined as:

$$L_{(p,q)}=\left\langle u^qu_L^{p-q-1}u_L'\right\rangle \quad (46)$$

and

$$T_{(p,q)}=\left(R_{(p,q+1)}-L_{(p,q)}\right)/2. \quad (47)$$

Figure 2 lists velocity correlation functions up to the sixth order. Just like second order correlations, all these correlation functions can be similarly computed from N-body simulations. We first identify all particle pairs with the same separation r, followed by a pairwised average to compute these correlations on a given scale r.

p	$q=0$	$q=1$	$q=2$	$q=3$	$q=4$	$q=5$
1	$L_{(1,0)}=\langle u_L^{'} \rangle$					
2	$L_{(2,0)}=\langle u_L u_L^{'} \rangle$	$R_{(2,1)}=\langle \mathbf{u}\cdot\mathbf{u}^{'} \rangle$				
3	$L_{(3,0)}=\langle u_L^2 u_L^{'} \rangle$	$R_{(3,1)}=\langle u_L \mathbf{u}\cdot\mathbf{u}^{'} \rangle$	$L_{(3,2)}=\langle u^2 u_L^{'} \rangle$			
4	$L_{(4,0)}=\langle u_L^3 u_L^{'} \rangle$	$R_{(4,1)}=\langle u_L^2 \mathbf{u}\cdot\mathbf{u}^{'} \rangle$	$L_{(4,2)}=\langle u^2 u_L u_L^{'} \rangle$	$R_{(4,3)}=\langle u^2 \mathbf{u}\cdot\mathbf{u}^{'} \rangle$		
5	$L_{(5,0)}=\langle u_L^4 u_L^{'} \rangle$	$R_{(5,1)}=\langle u_L^3 \mathbf{u}\cdot\mathbf{u}^{'} \rangle$	$L_{(5,2)}=\langle u^2 u_L^2 u_L^{'} \rangle$	$R_{(5,3)}=\langle u^2 u_L \mathbf{u}\cdot\mathbf{u}^{'} \rangle$	$L_{(5,4)}=\langle u^4 u_L^{'} \rangle$	
6	$L_{(6,0)}=\langle u_L^5 u_L^{'} \rangle$	$R_{(6,1)}=\langle u_L^4 \mathbf{u}\cdot\mathbf{u}^{'} \rangle$	$L_{(6,2)}=\langle u^2 u_L^3 u_L^{'} \rangle$	$R_{(6,3)}=\langle u^2 u_L^2 \mathbf{u}\cdot\mathbf{u}^{'} \rangle$	$L_{(6,4)}=\langle u^4 u_L u_L^{'} \rangle$	$R_{(6,5)}=\langle u^4 \mathbf{u}\cdot\mathbf{u}^{'} \rangle$

Figure 2. Velocity correlation functions of different order

4.2 Correlation functions in the limit $r \to 0$ and $r \to \infty$

We first identify the limiting ratio for odd order p (see Appendix A),

$$\lim_{r\to 0} \frac{\left\langle u^q u_L^{p-q-1} \right\rangle}{\left\langle u_L^{p-1} \right\rangle} = \frac{p}{p-q} \quad \text{with q=0...p-1}. \tag{48}$$

Equation (48) is also valid for $r \to \infty$ where velocity distributions are independent of scale r, i.e.

$$\lim_{r\to \infty} \frac{\left\langle u^q u_L^{p-q-1} \right\rangle}{\left\langle u_L^{p-1} \right\rangle} = \frac{p}{p-q} \quad \text{with q=0...p-1}. \tag{49}$$

Finally, using the definition of correlation functions (Eqs. (45)-(47)), for correlation functions of odd order p,

$$\lim_{r\to 0,\infty} \frac{L_{(p,q)}}{L_{(p,0)}} = \lim_{r\to 0,\infty} \frac{\left\langle u^q u_L^{p-q-1} \right\rangle}{\left\langle u_L^{p-1} \right\rangle} = \frac{p}{p-q}. \tag{50}$$

Similar relations can be obtained for correlation functions of even order p (from Eq. (49)),

$$\lim_{r\to 0} \frac{R_{(p,q+1)}}{L_{(p,0)}} = \lim_{r\to 0} \frac{\left\langle u^q u_L^{p-q-2} \mathbf{u}\cdot\mathbf{u}^{'} \right\rangle}{\left\langle u_L^{p-1} u_L^{'} \right\rangle} = \frac{p+1}{p-q-1}, \tag{51}$$

and

$$\lim_{r\to 0,\infty} \frac{L_{(p,q)}}{L_{(p,0)}} = \lim_{r\to 0,\infty} \frac{\left\langle u^q u_L^{p-q-1} u_L^{'} \right\rangle}{\left\langle u_L^{p-1} u_L^{'} \right\rangle} = \frac{p+1}{p+1-q}. \tag{52}$$

4.3 General kinematic relations for different types of flow

4.3.1 Kinematic relations for incompressible flow

For incompressible flow, the general kinematic relations for correlations of any order p are obtained as (see Appendix A4.3):

$$(p-q-1)\, R_{(p,q+1)} = \frac{1}{r^{p-q}} \left(r^{p-q+1} L_{(p,q)} \right)_{,r}, \tag{53}$$

$$2\,(p-q-1)\, T_{(p,q)} = \frac{1}{r} \left(r^2 L_{(p,q)} \right)_{,r}, \tag{54}$$

$$\left(r^2 R_{(p,q+1)} \right)_{,r} = \frac{2}{r^{p-q-1}} \left(r^{p-q+1} T_{(p,q)} \right)_{,r}. \tag{55}$$

4.3.2 Kinematic relations for constant divergence on small scale

For constant divergence flow on small scale, a general kinematic relation is obtained as (see Appendix A4.4):

$$(p-q-1)\, R_{(p,q+1)} + \left\langle u^q u_L^{p-q-1} \right\rangle \theta r = \frac{1}{r^{p-q}} \left(r^{p-q+1} L_{(p,q)} \right)_{,r}. \tag{56}$$

Equation (56) reduces to Eq. (53) for incompressible flow with $\theta = 0$.

For correlation functions of even order p (q is always an even number, see Eq. (56) and Fig. 2), we should have

$$\lim_{r\to 0} \left\langle u^q u_L^{p-q-1} \right\rangle = 0. \tag{57}$$

Therefore, here we can demonstrate that kinematic relations for even order correlations of constant divergence flow should be the same as that of incompressible flow. Equations (53)-(55) are still valid for correlations of even order p in constant divergence flow.

For odd order p, two special cases are considered here. With $q = p-1$ and $q = 0$ from Eq. (56), we should have relations

$$\left\langle u^{p-1} \right\rangle \theta r = \frac{1}{r} \left(r^2 L_{(p,p-1)} \right)_{,r} \tag{58}$$

and

$$(p-1)\, R_{(p,1)} + \left\langle u_L^{p-1} \right\rangle \theta r = \frac{1}{r^p} \left(r^{p+1} L_{(p,0)} \right)_{,r}. \tag{59}$$

For $r \to 0$, the correlation function $L_{(p,p-1)}$ can be directly solved from Eq. (58) that is proportional to r on small scale (Eq. (48)),

$$L_{(p,p-1)} = \frac{p}{3}\theta \left\langle u_L^{p-1} \right\rangle r = \frac{1}{3}\theta \left\langle u^{p-1} \right\rangle r. \tag{60}$$

For $p = 1$ and $q = 0$ in Eq. (59), the mean pairwise velocity (or first order structure function) $S_1^{lp}(r) = \langle \Delta u_L \rangle = \langle u_L^{'} - u_L \rangle = 2\langle u_L^{'} \rangle$ can be directly related to the divergence θ as

$$\theta = \frac{1}{2r^2} \left(r^2 \langle \Delta u_L \rangle \right)_{,r}. \tag{61}$$

With $\langle \Delta u_L \rangle = -Har$ from stable clustering hypothesis (Xu 2021d), the divergence on small scale $\theta = -3Ha/2$ can be obtained. Equation (61) is an important kinematic relation derived for constant divergence flow on small scale. However, it is actually valid for entire range of scales, as shown in Eq. (108), and will be repeatedly used in Section 6.

With Eq. (48), Eqs. (56) and (59), kinematic relations for odd order p should finally read

$$(p-q-1)\, R_{(p,q+1)} + \frac{1}{p-q}\frac{1}{r} \left(r^2 L_{(p,p-1)} \right)_{,r} = \frac{1}{r^{p-q}} \left(r^{p-q+1} L_{(p,q)} \right)_{,r}. \tag{62}$$

4.3.3 Kinematic relations for irrotational flow on large scale

For irrotational flow, kinematic relations of arbitrary order p and even number $0 \leqslant q \leqslant p-1$ are obtained as (see Appendix A4.5),

$$\left(R_{(p,q+1)} r \right)_{,r} + (p-q-2) L_{(p,q+2)} = \frac{1}{r^{p-q}} \left(r^{p-q+1} L_{(p,q)} \right)_{,r}, \tag{63}$$

$$(p-q)\, R_{(p,q+1)} - (p-q-2) L_{(p,q+2)} = \frac{2}{r^{p-q}} \left(r^{p-q+1} T_{(p,q)} \right)_{,r}, \tag{64}$$

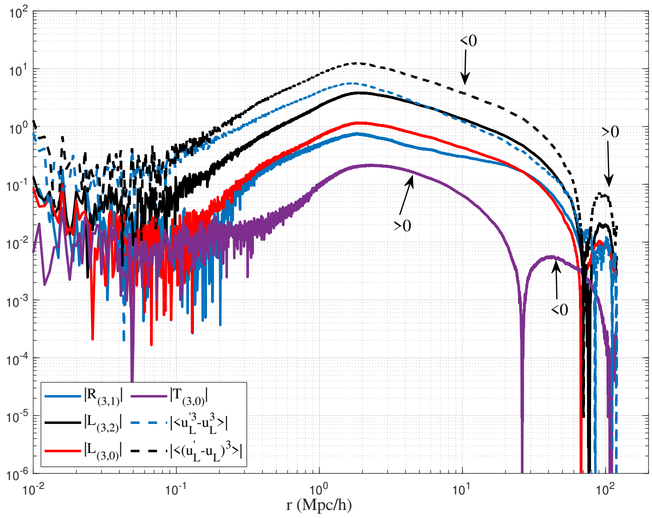

Figure 3. Two-point third order velocity correlation functions $L_{(3,0)}$, $R_{(3,1)}$, $L_{(3,2)}$, $T_{(3,0)}$, third moment of longitudinal velocity $-\langle u_L^{\prime 3}\rangle = \langle u_L^3\rangle$, and third order structure function $\langle (u_L^{\prime} - u_L)^3\rangle$ at z=0. All correlation functions are normalized by u^3, where u is the one-dimensional velocity dispersion of entire system. Only the transverse correlation $T_{(3,0)} > 0$ on small scale.

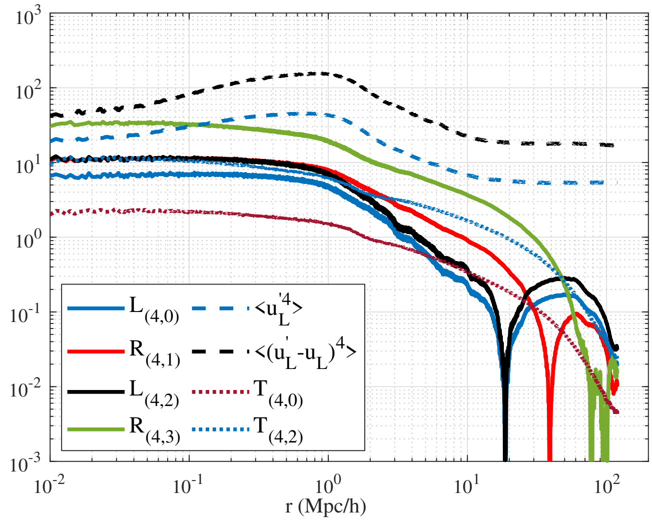

Figure 4. Two-point fourth order velocity correlation functions $L_{(4,0)}$, $R_{(4,1)}$, $L_{(4,2)}$, $R_{(4,3)}$, $T_{(4,0)}$, $T_{(4,2)}$, the fourth moment of longitudinal velocity $\langle u_L^{\prime 4}\rangle$, and fourth order structure function $\langle (u_L^{\prime} - u_L)^4\rangle$ at z=0. All correlation functions are normalized by u^4, where u is the one-dimensional velocity dispersion of entire system. The transverse correlation function $T_{(4,2)} > T_{(4,0)} > 0$ on small scale.

$$(p-q)\, L_{(p,q)} - (p-q-2)\, L_{(p,q+2)} = 2\left(rT_{(p,q)}\right)_{,r}. \qquad (65)$$

In Eqs. (63)-(65), terms involving correlation function $L_{(p,q+2)}$ should vanish if $q \geqslant p-2$.

5 RESULTS FROM N-BODY SIMULATIONS

This section presents the two-point velocity correlation and structure functions from N-body simulations. All statistical measures are computed in the same way as second order measures, where all particle pairs with a given separation r are identified first with particle velocities and locations recorded. Any statistical quantity on scale r is computed as the average of that quantity for all particle pairs with the same separation. The kinematic relations developed in Section 4 can be systematically verified by N-body simulation.

Figure 3 plots the variation of all third order correlation/structure functions and moment of longitudinal velocity with scale r at z=0. All correlation functions are normalized by u^3, where u is the one-dimensional velocity dispersion of entire system. All third order statistical measures vanish on both small and large scales and are negative with the only exception of transverse correlation $T_{(3,0)} > 0$.

Similarly, Fig. 4 presents the fourth order correlation/structure functions and moment at z=0 (normalized by u^4). All fourth statistical measures are positive on all scales and approaching constant in the limit of $r \to 0$ (small scale).

The general solution of correlation $L_{(p,p-1)}$ of odd order p on small scale (from Eq. (60)) is,

$$\frac{L_{(p,p-1)}}{u^p} = \frac{p}{3}\theta r \frac{\left\langle u_L^{p-1}\right\rangle}{u^p} = -2^{(p-3)/2} p K_{p-1}\left(u_L, 0\right) \frac{Har}{u}, \qquad (66)$$

where divergence $\theta = -3Ha/2$ and $\lim_{r\to 0}\langle u_L^2\rangle/u^2 = 2$ (see Xu 2022f, Fig. 22). The generalized kurtosis $K_{p-1}(u_L, r \to 0)$ of longitudinal velocity u_L can be found for the limiting X distribution of velocity from entropy maximization (Xu 2021c) and presented in a separate paper (see Xu 2022h, Table 3). Figure 5 presents the correlation functions $L_{(1,0)}$, $L_{(3,2)}$ and $L_{(5,4)}$ at z=0 (normalized by u, u^3, and u^5, respectively). The dash lines show solutions from Eq. (66).

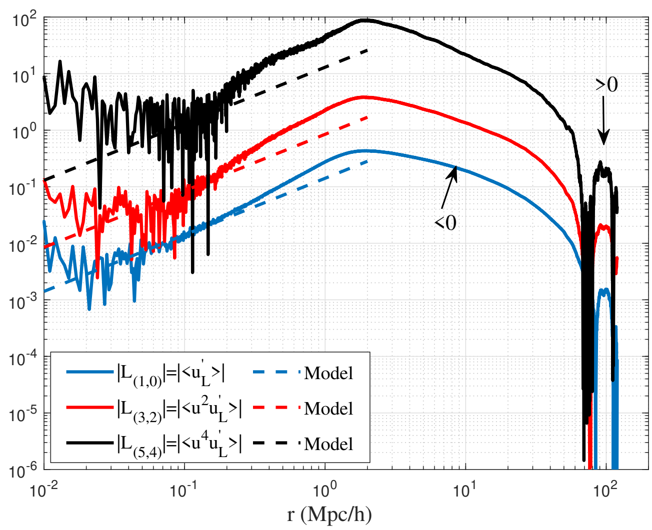

Figure 5. The variation of correlation functions $L_{(1,0)}$ (mean longitudinal velocity), $L_{(3,2)}$ and $L_{(5,4)}$ at z=0 (normalized by u, u^3, and u^5, respectively). The dash line shows the model from Eq. (66) on small scale.

For correlation functions of odd order p and even number q, kinematic relations for constant divergence flow on small scale in Eq.

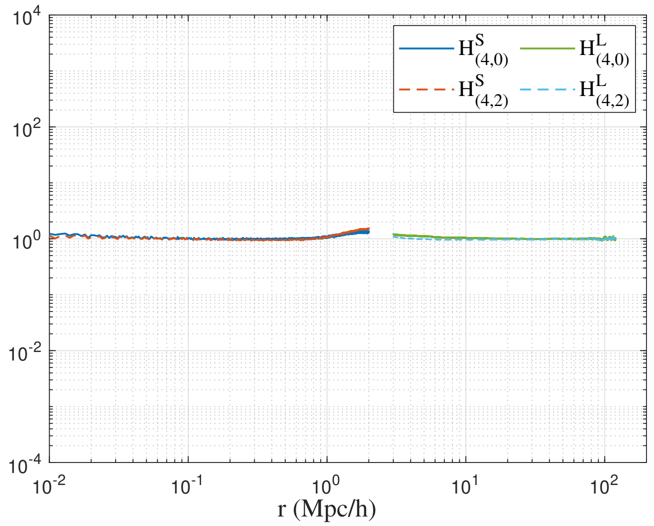

Figure 6. The variation of functions $H^S_{(4,0)}$ and $H^S_{(4,2)}$ (Eq. (68)) on small scale and $H^L_{(4,0)}$ and $H^L_{(4,2)}$ (Eq. (69)) on large scale from N-body simulation at z=0. Both functions are expected to be 1 from the kinematic relations for fourth order correlation functions.

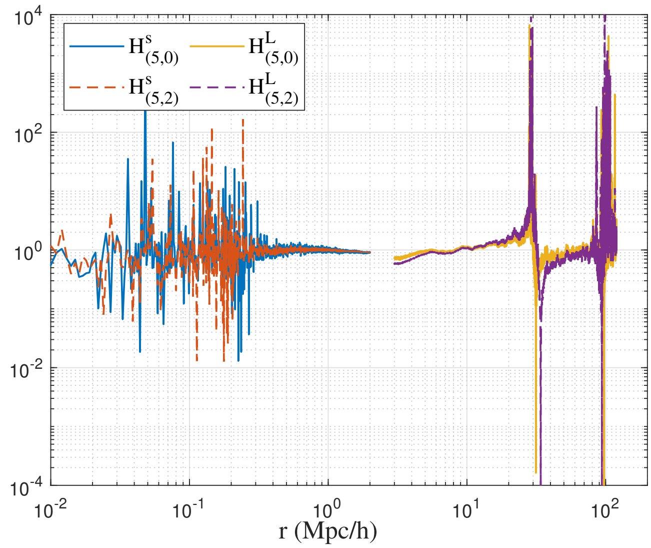

Figure 7. The variation of functions $H^S_{(5,0)}$ and $H^S_{(5,2)}$ (Eq. (67)) on small scale and $H^L_{(5,0)}$ and $H^L_{(5,2)}$ (Eq. (69)) on large scale from N-body simulation at z=0. Both functions are expected to be 1, as predicted by the kinematic relations for fifth order correlations.

(62) can be equivalently transformed to (integrating both sides)

$$H^S_{(p,q)}(r) = \frac{1}{(p-q)} \cdot \frac{L_{(p,p-1)}}{L_{(p,q)}} + \frac{(p-q-1)}{r^{p-q+1}L_{(p,q)}} \int_0^r \left(R_{(p,q+1)} - \frac{L_{(p,p-1)}}{p-q} \right) r^{p-q} dr = 1. \tag{67}$$

For correlation functions of even order p for constant divergence flow on small scale, kinematic relations are the same as incompressible flow (Eq. (56)) and can be similarly transformed to

$$H^S_{(p,q)}(r) = \frac{(p-q-1)}{r^{p-q+1}L_{(p,q)}} \int_0^r R_{(p,q+1)} r^{p-q} dr = 1. \tag{68}$$

Similarly, kinematic relations of any order p and even q for irrotational flow on large scale (Eq. (64)) can be transformed to

$$H^L_{(p,q)}(r) = \frac{1}{2r^{p-q+1}T_{(p,q)}} \int_0^r \left[(p-q) R_{(p,q+1)} - (p-q-2) L_{(p,q+2)} \right] r^{p-q} dr = 1. \tag{69}$$

Functions $H^S_{(p,q)}$ and $H^L_{(p,q)}$ are defined to verify the general kinematic relations and can be directly computed from N-body simulations. They are expected to be 1 on both small and large scales. Figures 6 and 7 plot the variation of functions $H^S_{(p,q)}$ on small scale and $H^L_{(p,q)}$ on large scale computed based on the fourth and fifth order correlation functions from N-body simulations. Both functions are expected to be 1 from kinematic relations for fourth and fifth order correlations, as shown in both Figures. These results valid our derivation for the general kinematic relations of any order.

6 DYNAMIC RELATIONS FROM DYNAMICS ON LARGE SCALE

So far, we have considered only kinematic relations, i.e. relations between correlation/structure functions of the same order (same p in Fig. 2). However, dynamic relations between correlation functions of different orders can only be determined from the dynamic evolution of velocity field, as shown in this and next sections.

The basic dynamics of self-gravitating collisionless flow (SG-CFD) follows from the collisionless Boltzmann equations (CBE), where the Jeans' equations on different order can be systematically constructed (Mo et al. 2010). However, the closure problem is well known for Jeans' equations which are not self-closed. The self-closed system of dynamic equations must be introduced on small and large scales, respectively. These dynamic equations are subsequently converted into the dynamic relations between correlation functions of different orders. This section focus on the dynamics on large scale. Section 7 focus on the dynamics on small scale.

6.1 Statistics from dynamics and the effective viscosity

On large scale, the peculiar velocity is of irrotational nature and can be expressed as the gradient of velocity potential. In literature, the dynamic equation for peculiar velocity $\mathbf{v}$ is usually modelled via an empirical "adhesion approximation" (Gurbatov et al. 1989; Buchert & Dominguez 2005),

$$\frac{\partial \mathbf{v}}{\partial t} + \frac{1}{a}\mathbf{v} \cdot \nabla \mathbf{v} = c(a)\mathbf{v} + \nu(a)\nabla^2 \mathbf{v}, \tag{70}$$

where $c(a)$ is a damping coefficient on large scale and $\nu(a)$ is an "artificial" viscosity in adhesion model. This section will attempt to elucidate the dynamic origin of "adhesion approximation" and the origin of "artificial" viscosity $\nu(a)$.

By neglecting the second order terms, we have the Zeldovich approximation on large scale from Eq. (70),

$$\frac{\partial \mathbf{v}}{\partial t} = c(a)\mathbf{v}. \tag{71}$$

For matter dominant cosmology with $H^2 = 8\pi G\rho_0/3$,

$$c(a) = \left(\frac{4\pi G\rho_0}{Hf(\Omega_m)} - H \right) = \frac{1}{2}H, \tag{72}$$

where $\rho_0(a)$ is the mean matter density. The adhesion approximation (a phenomenological model) extends the range of Zeldovich approximation into the weakly nonlinear regime.

The artificial ("effective") viscosity has its origin from inverse energy cascade (Eq. (97)) and nonlinear interaction of velocity fluctuations in SG-CFD (Eq. (156)). At this time, to develop dynamic relations, we adopt the adhesion approximation with a time-varying viscosity $\nu(a)$ as dominant dynamics on large scale.

Two identities can be introduced for arbitrary velocity field $\mathbf{u}$,

$$\mathbf{u}\cdot\nabla\mathbf{u} = \frac{1}{2}\nabla(\mathbf{u}\cdot\mathbf{u}) + (\nabla\times\mathbf{u})\times\mathbf{u}, \tag{73}$$

and

$$\nabla^2\mathbf{u} = \nabla(\nabla\cdot\mathbf{u}) - \nabla\times(\nabla\times\mathbf{u}). \tag{74}$$

For irrotational flow ($\nabla\times\mathbf{v}=0$) on large scale, this leads to

$$\mathbf{v}\cdot\nabla\mathbf{v} = \frac{1}{2}\nabla(\mathbf{v}\cdot\mathbf{v}) \quad \text{and} \quad \nabla^2\mathbf{v} = \nabla(\nabla\cdot\mathbf{v}), \tag{75}$$

such that the dynamic Eq. (70) can be rewritten as,

$$\frac{\partial\mathbf{v}}{\partial t} + \frac{1}{2a}\nabla(\mathbf{v}\cdot\mathbf{v}) = c(a)\mathbf{v} + \nu(a)\nabla^2\mathbf{v}. \tag{76}$$

The index notation of Eq. (76) at two different locations $\mathbf{x}$ and $\mathbf{x}'$ with a separation of r is

$$\frac{\partial v_j}{\partial t} + \frac{1}{2a}\frac{\partial(v_i v_i)}{\partial x_j} = c v_j + \nu\nabla^2 v_j, \tag{77}$$

$$\frac{\partial v_i'}{\partial t} + \frac{1}{2a}\frac{\partial\left(v_j' v_j'\right)}{\partial x_i'} = c v_i' + \nu\nabla'^2 v_i'. \tag{78}$$

Multiplying Eqs. (77) and (78) by v_i' and v_j respectively, adding two equations together, and taking the average on scale r lead to,

$$\begin{aligned}\frac{\partial\left\langle v_j v_i'\right\rangle}{\partial t} &+ \frac{1}{2a}\left\langle v_i'\frac{\partial(v_k v_k)}{\partial x_j} + v_j\frac{\partial\left(v_k' v_k'\right)}{\partial x_i'}\right\rangle \\ &= c\left\langle v_j v_i' + v_i' v_j\right\rangle + \nu\nabla^2\left\langle v_j v_i' + v_i' v_j\right\rangle,\end{aligned} \tag{79}$$

with the following facts being used,

(i) Velocity v_i' is independent of $\mathbf{x}$ and v_j is independent of $\mathbf{x}'$.
(ii) Partial derivatives $\partial/\partial x_j$ and $\partial/\partial x_i'$ can be replace by $-\partial/\partial r_j$ and $\partial/\partial r_i$, respectively, where $\partial/\partial x_i' = \partial/\partial r\cdot\hat{r}_i$ and $\partial/\partial x_j = -\partial/\partial r\cdot\hat{r}_j$, with unit vectors $\hat{r}_j = r_j/r$ and $\hat{r}_i = r_i/r$.
(iii) $\langle v_k v_k v_j'\rangle(\mathbf{r}) = \langle v_k' v_k' v_j\rangle(-\mathbf{r}) = -\langle v_k' v_k' v_j\rangle(\mathbf{r})$ from symmetry of third order tensor (see Eq. (2)).

From Eq. (79), the time evolution of second order correlation tensor Q_{ij} reads

$$\frac{\partial Q_{ij}}{\partial t} = \frac{1}{2a}\left(\frac{\partial Q_{kki}}{\partial r_j} + \frac{\partial Q_{kkj}}{\partial r_i}\right) + 2cQ_{ij} + 2\nu\nabla^2 Q_{ij}. \tag{80}$$

The dynamics of Q_{ij} is dependent on the third order correlation tensor Q_{kki}, which is dependent on the fourth order correlation tensor. Here we hit the closure problem.

Since the second order correlation function on large scale can be modelled explicitly (see Xu 2022f, Eq. (110)-(112)), third and higher order tensors can be obtained subsequently through the dynamic equation on large scale (see Eq. (80)). Multiplying both sides of Eq. (80) by δ_{ij} leads to the time evolution of second order correlation,

$$\frac{\partial R_2}{\partial t} = 2\Gamma(r) + 2cR_2 + 2\nu\left(\frac{1}{r^2}\frac{\partial}{\partial r}\left(r^2\frac{\partial R_2}{\partial r}\right)\right), \tag{81}$$

where the third order function $\Gamma(r)$ represents the energy transfer across scales due to the nonlinear advection term in Eq. (70). The energy transfer function $\Gamma(r)$ mimics the mass transfer function $T_m(m_h, a)$ for inverse mass cascade in halo mass space (see Xu 2021a, Eq. (18)). It describes the removal of kinetic energy from a small scale ($\Gamma(r) < 0$) and the deposition of kinetic energy at a larger scale ($\Gamma(r) > 0$). From Eq. (80), we should have

$$\Gamma(r) = \frac{1}{2a}\frac{\partial Q_{kki}}{\partial r_i}. \tag{82}$$

From definition of third order correlation tensor (Eqs. (1) and (5)),

$$Q_{kki} = Q_{jki}\delta_{jk} = \left(A_3 r^2 + 2B_3 + 3D_3\right)\hat{r}_i = R_{31}\hat{r}_i, \tag{83}$$

where $R_{31} = L_{(3,2)}$ in Fig. 2. From Eq. (15),

$$\frac{\partial Q_{kki}}{\partial r_i} = \frac{1}{r^2}\left(r^2 R_{31}\right)_{,r} \quad \text{and} \quad \Gamma(r) = \frac{1}{2ar^2}\left(r^2 R_{31}\right)_{,r}. \tag{84}$$

Substitution of $\Gamma(r)$ back to Eq. (81), an important dynamic relation between second order correlation $R_2(r)$ and third order correlation $R_{31}(r)$ are obtained. To derive an explicit expression for $R_{31}(r)$, the model of $R_2(r)$ can be used here (see Xu 2022f, Eq. (112)),

$$R_2(r) = \left\langle\mathbf{u}\cdot\mathbf{u}'\right\rangle = 2R(r) = a_0 u^2\exp\left(-\frac{r}{r_2}\right)\left(3 - \frac{r}{r_2}\right). \tag{85}$$

The comoving length scale r_2=23.13Mpc/h is a constant and might be related to the size of sound horizon r_s (see Xu 2022f, Eq. (122)). For a matter dominant model with $a_0 u^2 \propto a$ (see Xu 2022f, Fig. 20), we should have the time variation of $R_2(r)$,

$$\frac{\partial R_2}{\partial t} = \frac{\partial R_2}{\partial a}Ha = 2cR_2 = HR_2. \tag{86}$$

Substitution of Eq. (86) back to Eq. (81) leads to the relation between $R_2(r)$ and $R_{31}(r)$,

$$\frac{1}{r^2}\left(r^2 R_{31}\right)_{,r} + 2a\nu\left(\frac{1}{r^2}\frac{\partial}{\partial r}\left(r^2\frac{\partial R_2}{\partial r}\right)\right) = 0, \tag{87}$$

such that

$$L_{(3,2)}(r) = R_{31}(r) = -2a\nu\frac{\partial R_2}{\partial r}. \tag{88}$$

The density correlation $\xi(r)$ can be related to $R_2(r)$ as (see Xu 2022f, Eq. (120)),

$$\begin{aligned}\xi(r) &= -\frac{1}{(aHf(\Omega_m))^2}\left[\frac{1}{r^2}\frac{\partial}{\partial r}\left(r^2\frac{\partial R_2}{\partial r}\right)\right] \\ &= \frac{a_0 u^2/(rr_2)}{(aHf(\Omega_m))^2}\cdot\exp\left(-\frac{r}{r_2}\right)\left[\left(\frac{r}{r_2}\right)^2 - 7\left(\frac{r}{r_2}\right) + 8\right].\end{aligned} \tag{89}$$

The energy transfer function $\Gamma(r)$ can be related to density correlation $\xi(r)$ and reads (using Eq. (89) and (84))

$$\begin{aligned}\Gamma(r) &= \nu(aHf(\Omega_m))^2\xi(r) \\ &= \frac{\nu a_0 u^2}{rr_2}\exp\left(-\frac{r}{r_2}\right)\left[\left(\frac{r}{r_2}\right)^2 - 7\left(\frac{r}{r_2}\right) + 8\right].\end{aligned} \tag{90}$$

The third order total correlation function $R_{31}(r)$ can be related to the density correlation $\xi(r)$ as

$$\frac{1}{r^2}\left(r^2 R_{31}\right)_{,r} = 2a\nu\xi(r)(aHf(\Omega_m))^2. \tag{91}$$

From pair conservation Equation (see Xu 2022h, Eq. (47)), the mean pairwise velocity satisfies

$$\langle\Delta u_L\rangle \approx -\frac{2}{3}Har\bar{\xi}(r,a) = -\frac{2Ha}{r^2}\int_0^r \xi(y)y^2 dy \tag{92}$$

on large scale. Therefore, the mean pairwise velocity $\langle \Delta u_L \rangle$ can be modelled as (using Eqs. (85) and (89)),

$$\langle \Delta u_L \rangle = \frac{2}{aHf(\Omega_m)^2}\frac{\partial R_2}{\partial r} = \frac{2a_0 u^2}{aHr_2 f(\Omega_m)^2}\exp\left(-\frac{r}{r_2}\right)\left(\frac{r}{r_2}-4\right). \quad (93)$$

Using Eqs. (91) and (92), the relation between $R_{31}(r)$ and $\langle \Delta u_L \rangle$,

$$L_{(3,2)} = R_{31} = \left\langle u^2 u_L' \right\rangle = -\nu H a^2 f(\Omega_m)^2 \langle \Delta u_L \rangle = -\frac{2a_0 u^2 a\nu}{r_2}\exp\left(-\frac{r}{r_2}\right)\left(\frac{r}{r_2}-4\right), \quad (94)$$

which provides a simple model for third order correlation R_{31}.

Figure 8 plots the variation of $|R_{31}|$ with scale r at several different redshifts z. Without loss of generality, the correlation function R_{31} can be conveniently modelled as (based on Eq. (94))

$$L_{(3,2)} = R_{31} = \left\langle u^2 u_L' \right\rangle = a_3 u^3 \exp\left(-\frac{r}{r_2}\right)\left(\frac{r}{r_2}-b_3\right), \quad (95)$$

where coefficients a_3 and b_3 are obtained by fitting to the curves in Fig. 8. The viscosity $\nu(a)$ can be related to a_3 and a_0 (Eq. (94)),

$$a_3 = -\frac{2a_0 a\nu}{ur_2} \quad \text{or} \quad \alpha_\nu = -\frac{\nu}{u_0 r_2} = \frac{a_3 u}{2a_0 a u_0}, \quad (96)$$

i.e. the artificial viscosity in adhesion model (coefficient for momentum transport) is proportional to the typical velocity u and length scale r_2 ($\nu(a) \propto ur_2$, just like the viscosity of ideal gas, where r_2 is the mean free path).

In the standard K-epsilon turbulence model, the eddy viscosity is dependent on the kinetic energy and the rate of dissipation of kinetic energy. In SG-CFD for dark matter flow, the effective viscosity $\nu(a)$ on large scale can also be related to the kinetic energy and rate of energy production in SG-CFD,

$$\nu(a) = \frac{-1}{Ha^2 f(\Omega_m)^2}\frac{R_{31}}{\langle \Delta u_L \rangle} \quad \text{(from Eq. (94))}$$
$$\nu(a) = \frac{a_3 r_2}{3a_0 uat}\frac{\left(3u^2/2\right)^2}{\varepsilon_u} \approx \beta_\nu a^{1/2}\frac{\left(3u_0^2/2\right)^2}{\varepsilon_u} \sim a^{1/2}, \quad (97)$$

where $\varepsilon_u = -1.5du^2/dt \approx -1.5u_0^2/t_0$ is the rate of energy cascade and $3u^2/2$ is the specific kinetic energy of entire system. The constant $\beta_\nu \approx 4.9$ can be obtained from Fig. 12. By contrast, $\beta_\nu \approx 0.1$ in the standard K-epsilon turbulence model for incompressible flow.

The negative effective viscosity is a direct result of inverse energy cascade (Eq. (97)), where $\varepsilon_u < 0$, i.e. the kinetic energy is cascaded from smaller to larger mass sales. Plot of the effective viscosity in terms of coefficient α_ν in Eq. (96) is presented in Fig. 12.

The same model for $L_{(3,2)}$ in Eq. (95) can be generalized to high order correlation functions. Here we just present the models for the other two correlation functions along the diagonal in Fig. 2,

$$R_{(4,3)} = \left\langle u^2 \mathbf{u}\cdot\mathbf{u}' \right\rangle = a_4 u^4 \exp\left(-\frac{r}{r_2}\right)\left(b_4-\frac{r}{r_2}\right), \quad (98)$$

$$L_{(5,4)} = \left\langle u^4 u_L' \right\rangle = a_5 u^5 \exp\left(-\frac{r}{r_2}\right)\left(\frac{r}{r_2}-b_5\right). \quad (99)$$

Figures 8, 9, and 10 plot the variation of correlation functions $L_{(3,2)}$, $R_{(4,3)}$, and $L_{(5,4)}$ with scale r at different redshifts z. The model in Eqs. (95), (98) and (99) are also plotted in the same plots

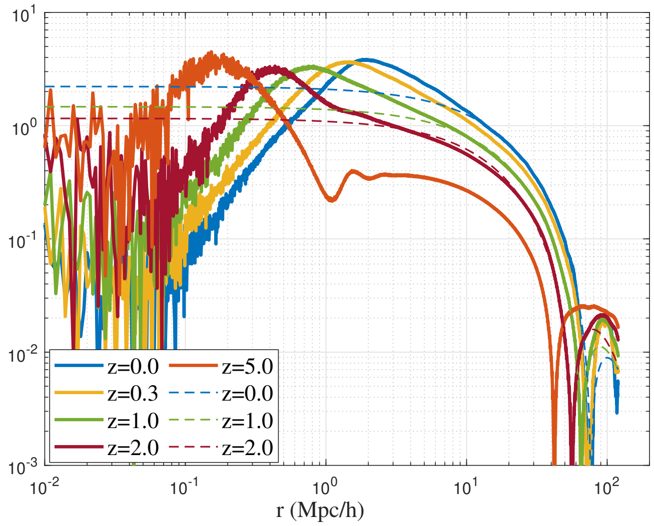

Figure 8. The variation of two-point third order velocity correlation function $R_{31} = L_{(3,2)}$ with scale r at different redshifts z (normalized by u^3). The model in Eq. (95) is also plotted in the same plot as dash lines.

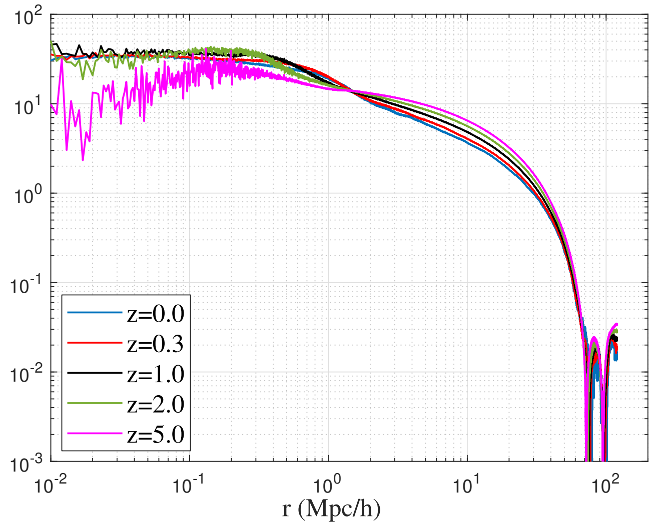

Figure 9. The variation of two-point fourth order velocity correlation function $R_{(4,3)}$ with scale r at different redshifts z (normalized by u^4). Model for $R_{(4,3)}$ is presented in Eq. (98).

as dash lines. Figure 11 plots the variation of correlation functions $R_{(2,1)}$, $R_{(4,3)}$, and $R_{(6,5)}$ with scale r at z=0. The dash line plots the model of $R_{(4,3)}$ from Eq. (98). Figure 12 plots the variation of coefficients a_m and b_m (m=3, 4, 5) for correlations $L_{(3,2)}$ (Eq. (95)), $R_{(4,3)}$ (Eq. (98)) and $L_{(5,4)}$ (Eq. (99)) with scale factor a.

It can be easily confirmed that $L_{(3,2)} \propto a^{5/2}$, $L_{(5,4)} \propto a^{7/2}$ and $R_{(4,3)} \propto a^2$. The viscosity coefficient $\nu(a) = -\alpha_\nu u_0 r_2 \propto a^{1/2}$, where $u_0 = 354.61km/s$ and $r_2 \approx 23.13Mpc/h$.

In principle, the same model can be generalized to any order (similar to the dynamic relation in Eq. (94)),

$$L_{(q+1,q)} = \left\langle u^q u_L' \right\rangle \propto u^q \left\langle u_L' \right\rangle \propto \left(\nu H a^2\right)^{q/2} L_{(1,0)} \propto a^{(q+3)/2}. \quad (100)$$

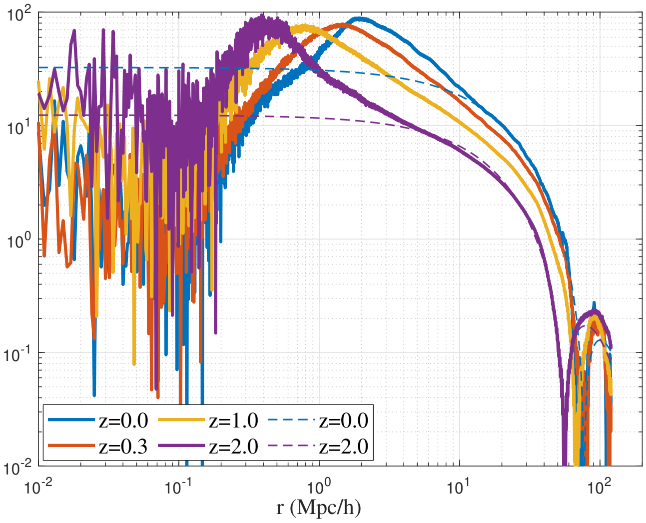

Figure 10. The variation of two-point fifth order velocity correlation function $L_{(5,4)}$ with scale r at different redshifts z (normalized by u^5). The model in Eq. (99) is also plotted in the same plot as dash lines.

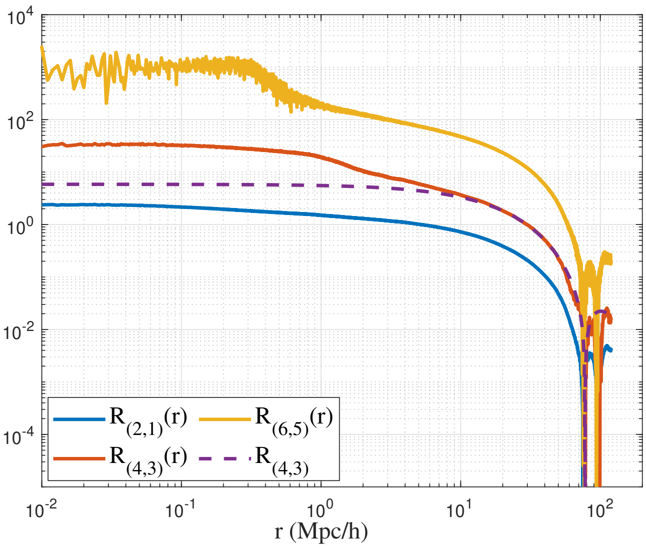

Figure 11. The variation of correlation functions $R_{(2,1)}$, $R_{(4,3)}$ and $R_{(6,5)}$ with scale r at z=0 (normalized by u^2, u^4, and u^6, respectively). The dash line shows the model from Eq. (98) for comparison.

The generalized dynamic relations (similar to Eq. (88)) between correlations of different order reads

$$L_{(q+1,q)} \propto -2a\nu \frac{\partial R_{(q,q-1)}}{\partial r}, \tag{101}$$

and

$$R_{(q,q-1)} = \left\langle u^{q-2}\mathbf{u}\cdot\mathbf{u}^{'}\right\rangle \propto u^{q-2}\left\langle \mathbf{u}\cdot\mathbf{u}^{'}\right\rangle \propto \left(\nu H a^2\right)^{(q-2)/2} R_{(2,1)} \propto a^{q/2}. \tag{102}$$

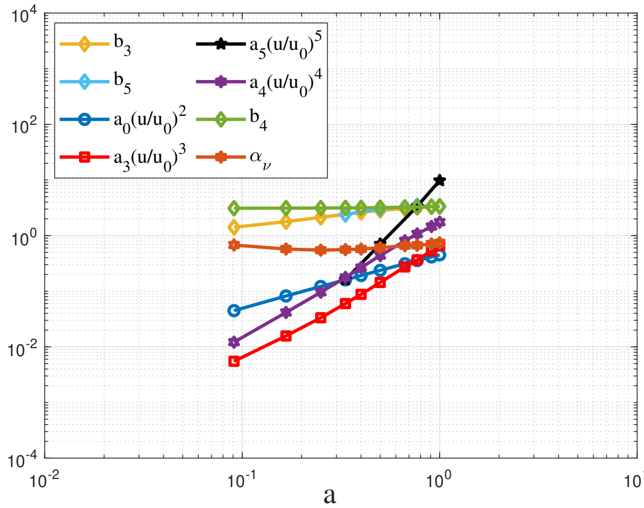

Figure 12. The variation of coefficients a_m and b_m (m=3, 4, 5) for velocity correlation functions $L_{(3,2)}$ (Eq. (95)), $R_{(4,3)}$ (Eq. (98)) and $L_{(5,4)}$ (Eq. (99)) with scale factor a. it can be confirmed that $a_0u^2 \propto a$, $a_3u^3 \propto a^{5/2}$, $a_4u^4 \propto a^2$ and $a_5u^5 \propto a^{7/2}$. The viscosity coefficient $\nu(a) = -\alpha_\nu u_0 r_2 \propto a^{1/2}$, where $u_0 = 354.61 km/s$ and $r_2 \approx 23 Mpc/h$. The negative viscosity reflects the inverse energy cascade from smaller to larger scales.

6.2 Dynamic relations between density correlation, mean density, and velocity dispersion

Just like the dynamic relations between third and second order statistics, the relation between second and first order statistics can be obtained by multiplying both sides of dynamic Eqs. (77) and (78) with unit vectors $\hat{r}_j = r_j/r$ and $\hat{r}_i = r_i/r$, respectively ($\mathbf{r} = \mathbf{x}^{'} - \mathbf{x}$),

$$\hat{r}_j \frac{\partial v_j}{\partial t} - \frac{1}{2a}\frac{\partial (v_i v_i)}{\partial r} = cu_L - \nu\frac{\partial}{\partial r}\left(\frac{\partial v_i}{\partial x_i}\right), \tag{103}$$

$$\hat{r}_i \frac{\partial v_i^{'}}{\partial t} + \frac{1}{2a}\frac{\partial \left(v_j^{'} v_j^{'}\right)}{\partial r} = cu_L^{'} + \nu\frac{\partial}{\partial r}\left(\frac{\partial v_j^{'}}{\partial x_j^{'}}\right). \tag{104}$$

Subtracting two equations and taking the average lead to,

$$\left\langle \hat{r}_i\frac{\partial v_i^{'}}{\partial t} - \hat{r}_j\frac{\partial v_j}{\partial t}\right\rangle + \frac{1}{a}\frac{\partial \left\langle u^2\right\rangle}{\partial r} = c\left\langle \Delta u_L\right\rangle + 2\nu\frac{\partial\langle\theta\rangle}{\partial r}, \tag{105}$$

where the pairwise velocity $\langle \Delta u_L\rangle = \langle u_L^{'} - u_L\rangle = \langle v_i^{'}\hat{r}_i - v_j\hat{r}_j\rangle$. The velocity dispersion $\langle u^2\rangle$ and divergence $\langle\theta\rangle$ on a given scale r are defined as

$$\left\langle u^2\right\rangle = \frac{1}{2}\left\langle |\mathbf{u}|^2 + \left|\mathbf{u}^{'}\right|^2\right\rangle \quad \text{and} \quad \langle\theta\rangle = \langle\nabla\cdot\mathbf{u}\rangle = \frac{1}{2}\left\langle \theta + \theta^{'}\right\rangle. \tag{106}$$

On large scale, the over-density can be related to divergence as (see Xu 2022f, Eq. (119)),

$$\delta \approx \eta = -\frac{\nabla\cdot\mathbf{u}}{aHf(\Omega_m)} = -\frac{\theta}{aHf(\Omega_m)}, \tag{107}$$

where $\eta(\mathbf{x}) = \log(1+\delta) \approx \delta$ is the log-density field. Function $f(\Omega_m)$ is dependent on the matter content Ω_m and $f(\Omega_m = 1) = 1$ for matter dominant model.

From identity in Appendix Eq. (A50) with $p = 1$ and $q = 0$ such that $\langle u_s^{'}\rangle = \langle u_L^{'}\hat{r}_s\rangle$ and taking the divergence on both sides leads to the relation between divergence $\langle\theta\rangle$ and pairwise velocity $\langle\Delta u_L\rangle$ on any scale r (using identity in Appendix Eq. (A6) and product rule for differentiation):

$$\langle\theta\rangle = \langle\nabla\cdot\mathbf{u}\rangle = \frac{1}{2r^2}\left(r^2\left\langle\Delta u_L\right\rangle\right)_{,r}. \tag{108}$$

This is an important kinematic relation good for entire range of scales. With Eq. (92) for $\langle\Delta u_L\rangle$ and Eq. (107) for δ, the divergence on scale r can be finally written as,

$$\langle\theta\rangle = \langle\nabla\cdot\mathbf{u}\rangle = -aHf\left(\Omega_m\right)\langle\delta\rangle = -Ha\xi\left(r\right). \tag{109}$$

Interestingly, the mean overdesnity at two locations separated by a comoving scale r can be related to the density correlation $\xi\left(r\right)$ on the same scale via a dynamic relation, i.e.

$$f\left(\Omega_m\right)\langle\delta\rangle = f\left(\Omega_m\right)\left\langle\delta+\delta^{'}\right\rangle/2 = \xi\left(r\right) = \left\langle\delta\delta^{'}\right\rangle, \tag{110}$$

where the first and second order statistics are connected via dynamics on large scale (Eq. (107)), the kinematic relation from Eq. (108), and the pair conservation equation (92).

Figure 13 plots the variation of both $\langle\delta\rangle$ and $\langle\delta\delta^{'}\rangle$ with scale r in a matter-dominant N-body simulation (Section 2), where $f\left(\Omega_m\right) = 1$ and $\langle\delta\rangle \approx \langle\delta\delta^{'}\rangle$ on large scale. With model of $\xi(r)$ proposed in Eq. (89) (see Xu 2022f, Eq. (121)), the variation of $\langle\delta\rangle$ on large scale should be known, where $\langle\delta\rangle < 0$ (the low density void region) for scales $r > 30Mpc/h$ (see Fig. 13).

Next, velocity dispersion on any scale of r can be related to the overdensity $\langle\delta\rangle$ on the same scale. In the linear regime, by neglecting the second order advection and viscous term, Eq. (70) reduces to Zeldovich approximation $\partial\mathbf{v}/\partial t = c\left(a\right)\mathbf{v}$ in Eq. (71). For velocity pair at $\mathbf{x}$ and $\mathbf{x}^{'}$ separated by $\mathbf{r}$, Eq. (71) leads to (multiplying $\hat{r}_i$)

$$\hat{r}_i\frac{\partial v_i}{\partial t} = c\left(a\right)\hat{r}_i v_i = c\left(a\right)u_L$$
and
$$\hat{r}_i\frac{\partial v_i^{'}}{\partial t} = c\left(a\right)\hat{r}_i v_i^{'} = c\left(a\right)u_L^{'}. \tag{111}$$

With Eqs. (111) and (109) for $\langle\theta\rangle$, the dynamic Eq. (105) gives

$$\begin{aligned}\frac{\partial\left\langle u^2\right\rangle}{\partial r} &= 2\nu a\frac{\partial\langle\theta\rangle}{\partial r}\\ &= -2\nu a^2Hf\left(\Omega_m\right)\frac{\partial\langle\delta\rangle}{\partial r} = -2\nu Ha^2\frac{\partial\xi\left(r\right)}{\partial r}.\end{aligned} \tag{112}$$

The velocity dispersion $\langle u^2\rangle$ on scale r can be related to the density correlation on the same scale as,

$$\left\langle u^2\right\rangle = 3u^2 - 2\nu Ha^2 f\left(\Omega_m\right)\langle\delta\rangle = 3u^2 - 2\nu Ha^2\xi\left(r\right),$$

or equivalently, a reduced velocity dispersion is

$$\frac{\left\langle u^2\right\rangle}{3u^2} - 1 = -\frac{2\nu Ha^2\xi\left(r\right)}{3u^2} = -\frac{2\nu Ha^2}{3u^2}f\left(\Omega_m\right)\langle\delta\rangle,$$

such that $\langle u^2\rangle$ can be analytically modelled (from Eq. (89)) as

$$\langle u^2\rangle = 3u^2 - \frac{2\nu}{Hf(\Omega_m)^2}\frac{a_0u^2}{rr_2}\cdot\exp\left(-\frac{r}{r_2}\right)\left[\left(\frac{r}{r_2}\right)^2 - 7\left(\frac{r}{r_2}\right) + 8\right], \tag{113}$$

where the overdensity $\langle\delta\rangle$ on scale r is proportional to a reduced velocity dispersion on the same scale. For $r \to \infty$, $\langle u^2\rangle = 3u^2$ and $\langle\delta\rangle = 0$ (see Xu 2022h, Fig. 20).

In practice, the particle overdensity in N-body simulation can be obtained using Delaunay tessellation (Xu 2022h). Figure 13 also plots the variation of reduced velocity dispersion $\left\langle u^2\right\rangle/\left(3u^2\right)-1$ with scale r that is proportional to density correlation or mean overdensity, i.e. $\propto\xi\left(r\right)$ or $\propto\langle\delta\rangle$ from Eq. (113).

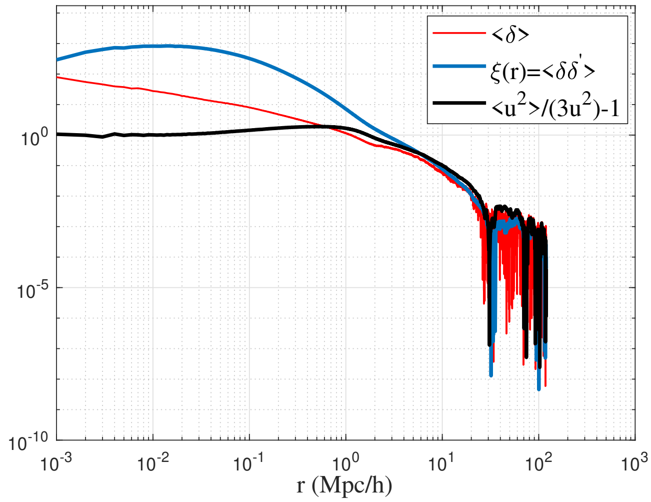

Figure 13. The variation of density correlation $\xi\left(r\right) = \langle\delta\delta^{'}\rangle$ and average over-density $\langle\delta\rangle = \langle\delta+\delta^{'}\rangle/2$ with scale r from N-body simulation at z=0. A relation between first and second order statistics $\langle\delta\rangle \approx \langle\delta\delta^{'}\rangle$ on large scale (Eq. (110)) can be identified. The plot also shows the relation between a reduced velocity dispersion and density correlation on large sale, i.e. $\langle u^2\rangle/(3u^2) - 1 \propto \xi\left(r\right) \propto \langle\delta\rangle$ from Eq. (113). The lower overdensity leads to the smaller velocity dispersion.

Fianlly, an equation for the evolution of transverse velocity $\mathbf{v}_T$ may be obtained. On large scale at a given scale r, using the product rule of differentiation for $u_L = v_i\hat{r}_i$ and Eq. (111),

$$\frac{\partial u_L}{\partial t} = v_i\frac{\partial\hat{r}_i}{\partial t} + \hat{r}_i\frac{\partial v_i}{\partial t} = v_i\frac{\partial\hat{r}_i}{\partial t} + c\hat{r}_iv_i = v_i\frac{\partial\hat{r}_i}{\partial t} + cu_L. \tag{114}$$

From Eq. (93) for pairwise velocity $\langle\Delta u_L\rangle$, we would expect that

$$\frac{\partial\left\langle u_L\right\rangle}{\partial t} = \left(1 - \frac{\partial\ln\dot{a}}{\partial\ln a}\right)H\left\langle u_L\right\rangle. \tag{115}$$

Combining Eq. (115) with Eq. (114), we should have

$$\left\langle v_i\frac{\partial\hat{r}_i}{\partial t}\right\rangle = \left[\left(1 - \frac{\partial\ln\dot{a}}{\partial\ln a}\right)H - c\left(a\right)\right]\left\langle u_L\right\rangle. \tag{116}$$

Use the definition of transverse velocity in Eq. (10) and Eq. (111),

$$\left\langle\frac{\partial\mathbf{v}_T}{\partial t}\cdot\hat{\mathbf{r}}\right\rangle = -\left\langle\mathbf{v}\cdot\frac{\partial\hat{\mathbf{r}}}{\partial t}\right\rangle, \tag{117}$$

which is the acceleration of transverse velocity projecting along the $\hat{\mathbf{r}}$ vector (centripetal acceleration).

On large scale, the (first order) peculiar velocity satisfies (Zeldovich approximation in Eq. (71)) $\partial\mathbf{v}/\partial t = c\left(a\right)\mathbf{v}$, while the transverse velocity $\mathbf{v}_T$ should satisfy,

$$\begin{aligned}\left\langle\mathbf{v}\cdot\frac{\partial\hat{\mathbf{r}}}{\partial t}\right\rangle &= -\left\langle\frac{\partial\mathbf{v}_T}{\partial t}\cdot\hat{\mathbf{r}}\right\rangle\\ &= \left[\left(1 - \frac{\partial\ln\dot{a}}{\partial\ln a}\right)H - c\left(a\right)\right]\langle\mathbf{v}\cdot\hat{\mathbf{r}}\rangle \approx H\left\langle u_L\right\rangle \propto a^0.\end{aligned} \tag{118}$$

6.3 Exponential and power-law velocity correlations on large and small scales

The exponential function was proposed for second order transverse velocity correlation $T_{(2,0)} \propto ae^{-r/r_2}$ on large scale (see Xu 2022f,

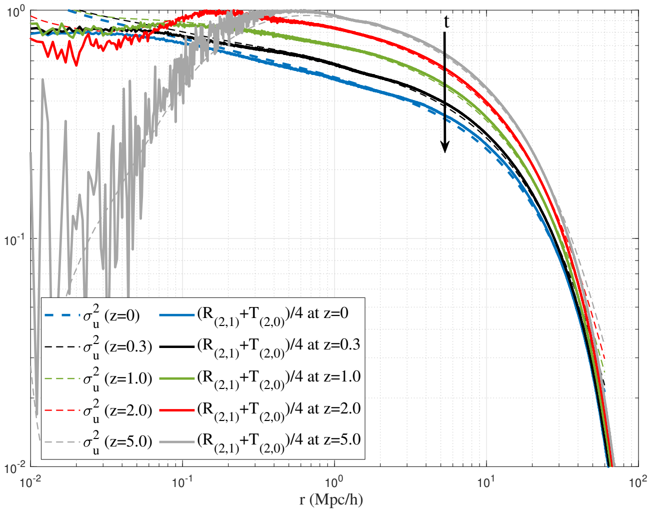

Figure 14. The variation of velocity dispersion $\sigma_u^2(r)$ (kinetic energy contained in scales above r) with scale r at different redshifts z. Function $\sigma_u^2(r)$ is obtained from N-body simulation using Eq. (119). Approximation of $\sigma_u^2(r)$ by correlations (Eq. (121)) is also presented as solid lines for comparison.

Eq. (110)). This is not a coincidence and must be deeply rooted in the dynamics and kinematics on large scale, which is demonstrated in this section.

We first look at the distribution of kinetic energy on different scales via one-dimensional variance of smoothed velocity (the bulk flow) using a spherical filter of radius r, i.e. velocity dispersion functions $\sigma_u^2(r)$ and $\sigma_d^2(r)$ for kinetic energy contained in all scales above or below r (see Xu 2022f, Eqs. (27) and (29)),

$$\sigma_u^2(r) = \frac{1}{3}\int_{-\infty}^{\infty} E_u(k)\, W(kr)^2\, dk$$

and (119)

$$\sigma_d^2(r) = \frac{1}{3}\int_{-\infty}^{\infty} E_u(k)\left[1 - W(kr)^2\right] dk,$$

where $W(x \equiv kr)$ is a window function. For a tophat spherical filter, the window function $W(x)$ reads

$$W(x) = \frac{3}{x^3}\left[\sin(x) - x\cos(x)\right] = 3\frac{j_1(x)}{x}, \tag{120}$$

where $j_1(x)$ is the *first* order spherical Bessel function of *first* kind.

On large scale, dispersion function $\sigma_u^2(r)$ is well approximated by $R_{(2,1)}(r)$ and $T_{(2,0)}(r)$ as

$$\sigma_u^2(r) \approx \frac{1}{4}\left[R_{(2,1)}(r) + T_{(2,0)}(r)\right], \tag{121}$$

which is a manifestation of energy equipartition including three translational degrees of freedom in total correlation $R_{(2,1)}$ and one rotational degree of freedom in transverse correlation $T_{(2,0)}$. Correlations on large scale characterize the motion of halos. For pair of halos, transverse motion is dominant. The longitudinal correlation is relatively small on large scale and can be neglected. Figure 14 plots the variation of velocity dispersion $\sigma_u^2(r)$ at different redshifts z. Function $\sigma_u^2(r)$ is obtained directly from N-body simulation (also see Xu 2022f, Fig. 9). The approximation of $\sigma_u^2(r)$ by Eq. (121) is also presented as solid lines with good agreement.

While correlations on small scale reflect the motion of particles in the same halo such that longitudinal correlation is comparable to transverse correlation (see Xu 2022f, Figs. 3 and 4). Therefore, the velocity dispersion function $\sigma_u^2(r)$ can be approximated by

$$\sigma_u^2(r) \approx \frac{1}{5}\left[R_{(2,1)}(r) + T_{(2,0)}(r) + L_{(2,0)}(r)\right], \tag{122}$$

with an additional degree of freedom from longitudinal correlation. When combined with kinematic relations for constant divergence flow on small scale (see Xu 2022f, Eqs. (138)-(141)), Equation (122) can be used to derive the power-law correlation functions on small scale, i.e. $\sigma_d^2(r) \propto r^n$. Equation for exponent n of power-law can be easily obtained as,

$$(10 + 3n)(4 + n)(6 + n) = 15 \cdot 2^{n+4}, \tag{123}$$

which gives $n \approx 1/4$ and provides the dynamic and kinematic origin of the "one-fourth" law for constant divergence flow on small scale (see Xu 2022f, Section 5.2).

Next, the total enstrophy contained in all scales below r can be related to third order correlation function $L_{(3,2)}(r)$. From dynamic relations on large scale (Eq. (88)) and the Fourier transform of total correlation $R_{(2,1)}(r)$,

$$R_{(2,1)}(r) = 2\int_0^{\infty} E_u(k)\frac{\sin(kr)}{kr}dk,$$

the Fourier transform of $L_{(3,2)}(r)$ can be obtained as, (124)

$$L_{(3,2)}(r) = -2a\nu\frac{\partial R_{(2,1)}}{\partial r} = 4a\nu\int_0^{\infty} E_u(k)\, j_1(kr)\, k\, dk,$$

With $j_1(x) \approx x/3 - x^3/30$ for small $x = kr$, we can write (using definition in Eq. (119))

$$\frac{L_{(3,2)}(r)}{ar} \approx \frac{20}{3}\nu\left[\frac{1}{r^2}\int_0^{\infty} E_u(k)\left(1 - W^2(kr)\right)dk\right] = \frac{20}{3}\nu\underbrace{\frac{\sigma_d^2(r)}{r^2}}_{1}, \tag{125}$$

where term 1 represents the mean square strain rate (or velocity gradient) below scale r. Therefore, the RHS term (multitplied by the viscosity) represents the rate of energy cascaded at scale r.

In addition, the structure function $S_2^x(r)$ is introduced for enstrophy in our previous work (see Xu 2022f, Eq. (73)),

$$\frac{S_2^x(r)}{2r^2} = \frac{1}{3}\int_0^{\infty} E_u(k)\, k^2 W^2(kr)\, dk, \tag{126}$$

which represents the one-dimensional enstrophy contained in all scales above r. With both Eqs. (125) and (126), the third order correlation $L_{(3,2)}(r)$ is proportional to $S_2^x(r)$,

$$\frac{L_{(3,2)}(r)}{ar} \approx 4\nu\frac{S_2^x(r)}{2r^2}, \tag{127}$$

which represents the rate of an inverse energy transfer from scales below r to scales above r. Figure 15 plots the variation of both functions in Eq. (127) with scale r at different z, where $L_{(3,2)}(r)$ can be related to the enstrophy contained in scales above r.

The rate of energy transfer can also be expressed in terms of kinetic energy $\sigma_u^2(r)$ divided by the turnaround time $(ar)/u$ on scale r, where u^2 is the one-dimensional velocity dispersion of entire system. Finally, we can write the relations (with Eq. (121))

$$-\frac{L_{(3,2)}(r)}{ar} \approx \alpha_r\frac{\sigma_u^2(r)}{(ar)/u} = \frac{\alpha_r}{4}\left[R_{(2,1)}(r) + T_{(2,0)}(r)\right]\frac{u}{ar}, \tag{128}$$

where α_r is a proportional constant and $L_{(3,2)}(r) < 0$. With dynamic

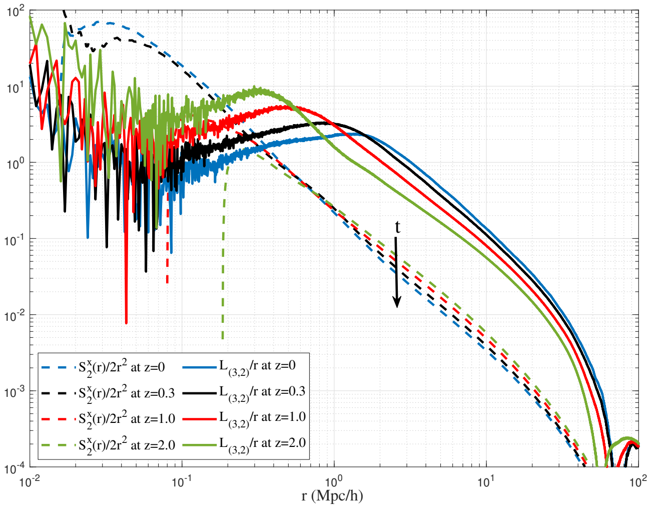

Figure 15. Comparison between structure function $S_2^x(r)/(2r^2)$ and third order correlation function $L_{(3,2)}(r)/r$. On large scale, $L_{(3,2)}(r)$ is related to the enstrophy contained in all scales above r or the rate of energy transfer from scale below r to scale above r.

relations (Eq. (88)) on large scale, Eq. (128) becomes

$$\frac{8\nu a}{\alpha_r u}\frac{\partial R_{(2,1)}}{\partial r} = \left[R_{(2,1)}(r) + T_{(2,0)}(r)\right]. \tag{129}$$

Using the kinematic relation between $R_{(2,1)}$ and $T_{(2,0)}$ in Eq. (A19) (or see Xu 2022f, Eq. (47)) for second order correlations on large scale for irrotational flow, the exponential form of transverse correlation function can be fully recovered, where

$$T_{(2,0)} = Const \cdot \exp\left(-\frac{r}{r_2}\right) \quad \text{with} \quad r_2 = -\frac{8\nu a}{\alpha_r u}. \tag{130}$$

Comparing with Eq. (96), we found constant $\alpha_r \equiv 4a_3/a_0 \propto a^{3/4}$.

7 DYNAMIC RELATIONS ON SMALL SCALE

7.1 Dynamic equations for velocity on small scale

To author's knowledge, self-closed equations for velocity evolution on small scale do not exist. In this section, we will first formulate the self-close equations for velocity. These equations are subsequently applied to derive dynamic relations on small scale.

7.1.1 *Self-closed dynamic equations for velocity*

On small scale, the flow is of constant divergence, i.e. $\nabla\cdot\mathbf{v} = \theta$. We focus on the momentum equation (Jeans' equation) for peculiar velocity in comoving coordinate,

$$\frac{\partial\mathbf{v}}{\partial t} + \frac{1}{a}\mathbf{v}\cdot\nabla\mathbf{v} + H\mathbf{v} = -\frac{1}{a}\frac{\nabla\cdot\mathbf{p}}{\rho} - \frac{1}{a}\nabla\phi, \tag{131}$$

where $\mathbf{p} = \rho\boldsymbol{\sigma}^2$ is the pressure tensor, $\boldsymbol{\sigma}^2$ is the velocity dispersion tensor, and ϕ is the gravitational potential.

It is well known that this equation is not closed, and closure must be developed. Starting from the halo-based description of entire system, peculiar velocity can be decomposed into velocity due to the motion of halos ($\mathbf{v}_h$) and velocity due to the motion in halos, i.e. intra-halo motion $\mathbf{v}_\nu$ (also see Xu 2021f, Eq. (14)),

$$\mathbf{v}(\mathbf{x},t) = \mathbf{v}_h(\mathbf{x}_h,t) + \mathbf{v}_\nu(\mathbf{r},t), \tag{132}$$

where $\mathbf{x}_h$ is the center of mass of a given halo and $\mathbf{r}$ is the vector relative to the halo center such that particle position $\mathbf{x} = \mathbf{x}_h + \mathbf{r}$. All particles in the same halo should have the same halo velocity $\mathbf{v}_h$. The spatial variation of $\mathbf{v}_h$ is on a much larger length scale, compared to the variation of $\mathbf{v}_\nu$. Therefore, $\mathbf{v}_h$ is relatively a constant on halo scale. The motion in halo (velocity $\mathbf{v}_\nu$) can be further decomposed into the radial flow and azimuthal flow, where polar flow can be neglected (see Xu 2022e, Fig. 2),

$$\mathbf{v}_\nu = \mathbf{v}_r + \mathbf{v}_\varphi. \tag{133}$$

In spherical coordinate, the mean (peculiar) radial flow and azimuthal flow for virilized halos are obtained as (see solutions for small halos with low peak height ν) (see Xu 2022e, Section 3.4),

$$\mathbf{v}_r = -Ha\mathbf{r}, \quad \mathbf{v}_\varphi = \boldsymbol{\omega}_h\times\mathbf{r}, \quad \text{and} \quad \boldsymbol{\omega}_h = \left(\nabla\times\mathbf{v}_\varphi\right)/2. \tag{134}$$

where $\boldsymbol{\omega}_h$ is the angular velocity of that halo and should be the same for all particles in the same halo. Obviously, the radial and azimuthal flow have the following properties:

$$\begin{aligned}&\nabla\mathbf{v}_r = -Ha\nabla\mathbf{r} = -Ha\mathbf{I}, \quad \nabla\mathbf{v}_\varphi + \left(\nabla\mathbf{v}_\varphi\right)^T = 0,\\ &\nabla\times\mathbf{v}_r = 0, \quad \text{and} \quad \mathbf{v}_\varphi = \mathbf{r}\cdot\nabla\mathbf{v}_\varphi,\end{aligned} \tag{135}$$

where $\mathbf{I}$ is an identity matrix and $\nabla\mathbf{v}_\varphi$ is antisymmetric. It can be easily confirmed that the radial flow satisfies (from Eq. (135))

$$\frac{\partial\mathbf{v}_r}{\partial t} + \frac{1}{a}\mathbf{v}_r\cdot\nabla\mathbf{v}_r + H\mathbf{v}_r = \frac{\partial\mathbf{v}_r}{\partial t}, \tag{136}$$

and the azimuthal flow satisfies (from Eq. (134))

$$H\mathbf{v}_\varphi + \frac{1}{a}\boldsymbol{\omega}_h\times\mathbf{v}_r = 0. \tag{137}$$

Radial and azimuthal flow in Eq. (134) also satisfy the following three equations,

$$\frac{1}{a}\mathbf{v}_\varphi\cdot\nabla\mathbf{v}_r + H\mathbf{v}_\varphi = 0 \quad \text{(from Eq. (135))}, \tag{138}$$

$$\frac{1}{a}\mathbf{v}_r\cdot\nabla\mathbf{v}_\varphi = \frac{1}{a}\boldsymbol{\omega}_h\times\mathbf{v}_r \quad \text{(from Eq. (135))}, \tag{139}$$

$$\frac{\partial\mathbf{v}_\varphi}{\partial t} + \frac{1}{a}\mathbf{v}_\varphi\cdot\nabla\mathbf{v}_\varphi = \frac{1}{a}\boldsymbol{\omega}_h\times\mathbf{v}_\varphi \quad \text{(Newton's second law)}. \tag{140}$$

By adding Eqs. (136), (138), (139) and (140) together, the equation for intra-halo motion $\mathbf{v}_\nu$ is,

$$\begin{aligned}\frac{\partial\mathbf{v}_\nu}{\partial t} + \frac{1}{a}\mathbf{v}_\nu\cdot\nabla\mathbf{v}_\nu + H\mathbf{v}_\nu &= \frac{\partial\mathbf{v}_r}{\partial t} + \frac{1}{a}\boldsymbol{\omega}_h\times\mathbf{v}_\nu\\ &= \frac{\partial\mathbf{v}_r}{\partial t} + \frac{1}{2a}\left(\nabla\times\mathbf{v}_\nu\right)\times\mathbf{v}_\nu.\end{aligned} \tag{141}$$

The motion of halo $\mathbf{v}_h$ is spatially varying on a much larger scale than the size of halo, i.e. the motion of halo $\mathbf{v}_h$ can be treated as a constant on halo scale such that

$$\frac{1}{a}\mathbf{v}_\nu\cdot\nabla\mathbf{v}_h \approx 0 \quad \text{and} \quad \frac{1}{a}\mathbf{v}_h\cdot\nabla\mathbf{v}_h \approx 0. \tag{142}$$

In addition, using the identity for two vectors $\mathbf{A}$ and $\mathbf{B}$,

$$\mathbf{A}\times(\nabla\times\mathbf{B}) = \mathbf{A}\cdot\left[(\nabla\mathbf{B})^T - \nabla\mathbf{B}\right], \tag{143}$$

halo velocity $\mathbf{v}_h$ satisfies ($\nabla \mathbf{v}_\varphi$ is antisymmetric and Eq. (135))

$$\mathbf{v}_h \cdot \nabla \mathbf{v}_\varphi = \boldsymbol{\omega}_h \times \mathbf{v}_h \quad \text{and} \quad \frac{1}{a}\mathbf{v}_h \cdot \nabla \mathbf{v}_r + H\mathbf{v}_h = 0. \tag{144}$$

Equation for $\mathbf{v}_h$ is finally written as (using Eqs. (134) and (144)),

$$\begin{aligned}\frac{\partial \mathbf{v}_h}{\partial t} + \frac{1}{a}\mathbf{v}_h \cdot \nabla \mathbf{v}_v + H\mathbf{v}_h &= \frac{\partial \mathbf{v}_h}{\partial t} + \frac{1}{a}\mathbf{v}_h \cdot \nabla \mathbf{v}_\varphi \\ &= \frac{\partial \mathbf{v}_h}{\partial t} + \frac{1}{2a}\left(\nabla \times \mathbf{v}_\varphi\right) \times \mathbf{v}_h.\end{aligned} \tag{145}$$

Adding Eq. (141) for intra-halo motion $\mathbf{v}_v$ and Eqs. (142) and (145) for motion of halo $\mathbf{v}_h$ together with the relation $\nabla \times \mathbf{v}_\varphi = \nabla \times \mathbf{v}_v = \nabla \times \mathbf{v}$, the dynamic equation for total particle velocity $\mathbf{v}$ reads,

$$\frac{\partial \mathbf{v}}{\partial t} + \frac{1}{a}\mathbf{v} \cdot \nabla \mathbf{v} + H\mathbf{v} = \frac{\partial \mathbf{v}_r}{\partial t} + \frac{\partial \mathbf{v}_h}{\partial t} + \frac{1}{2a}\left(\nabla \times \mathbf{v}\right) \times \mathbf{v}. \tag{146}$$

With $\nabla \times \mathbf{v}_h = 0$ and $\nabla \times \mathbf{v}_r = 0$, both $\mathbf{v}_r$ and $\mathbf{v}_h$ are of irrotational nature that can be expressed as gradient of a scalar field (velocity potential) such that

$$\begin{aligned}\frac{\partial \mathbf{v}_r}{\partial t} + \frac{\partial \mathbf{v}_h}{\partial t} &= -\frac{1}{a}\left(\frac{\partial \nabla \phi_r}{\partial t} + \frac{\partial \nabla \phi_h}{\partial t}\right) \\ &= -\frac{1}{a}\nabla \frac{\partial}{\partial t}\left(\phi_r + \phi_h\right) = -\frac{1}{a}\nabla \phi^*,\end{aligned} \tag{147}$$

where ϕ_r and ϕ_h are the velocity potential for intra-halo radial flow $\mathbf{v}_r$ and halo motion $\mathbf{v}_h$ and total potential $\phi^* = \partial(\phi_r + \phi_h)/\partial t$.

The final complete set of self-closed dynamic equations reads,

$$\nabla \cdot \mathbf{v} = \theta\left(t\right)$$

and

$$\frac{\partial \mathbf{v}}{\partial t} + \frac{1}{a}\mathbf{v} \cdot \nabla \mathbf{v} + H\mathbf{v} = -\frac{1}{a}\nabla \phi^* + \gamma \frac{1}{a}\underbrace{\left(\nabla \times \mathbf{v}\right) \times \mathbf{v}}_{1}, \tag{148}$$

where we have four equations for velocity $\mathbf{v}$ and potential ϕ^* with a constant (in space) divergence $\theta = -3Ha/2$ (see Eq. (61)).

Here coefficient γ is dependent on the scale and halo properties (virialized or not). For velocity on small scale $\gamma = 1/2$ (comparing Eqs. (148) and (146)), and in principle, γ can be determined from simulation (Fig. 16). Term 1 stands for the centripetal acceleration from pressure gradient due to velocity dispersion (Eq. (131)). With appropriate boundary and initial conditions, Eq. (148) is self-closed and can be numerically solved for velocity field $\mathbf{v}$ and potential field ϕ^*. Using identity

$$\nabla \cdot \left(\mathbf{v} \otimes \mathbf{v}\right) = \mathbf{v}\left(\nabla \cdot \mathbf{v}\right) + \mathbf{v} \cdot \nabla \mathbf{v}, \tag{149}$$

and identity in Eq. (73), Eq. (148) can be equivalently transformed to other forms for the convenience of numerical solution,

$$\frac{\partial \mathbf{v}}{\partial t} + \frac{1}{a}\left(1-\gamma\right)\mathbf{v} \cdot \nabla \mathbf{v} + \frac{\gamma}{2a}\nabla\left(\mathbf{v} \cdot \mathbf{v}\right) + H\mathbf{v} = -\frac{1}{a}\nabla \phi^*, \tag{150}$$

and

$$\begin{aligned}&\frac{\partial \mathbf{v}}{\partial t} + \frac{1}{a}\left(1-\gamma\right)\nabla \cdot \left(\mathbf{v} \otimes \mathbf{v}\right) \\ &\quad + \frac{\gamma}{2a}\nabla\left(\mathbf{v} \cdot \mathbf{v}\right) + \left[H - \frac{1}{a}\left(1-\gamma\right)\theta\right]\mathbf{v} = -\frac{1}{a}\nabla \phi^*.\end{aligned} \tag{151}$$

Please note that by setting $\gamma = 1$ and

$$\nabla \phi^* = -\frac{3}{2}Ha\mathbf{v} - a\nu\nabla^2\mathbf{v} = -\frac{3}{2}Ha\mathbf{v} - a\nu\nabla\left(\nabla \cdot \mathbf{v}\right), \tag{152}$$

Eqs. (150) and (151) reduces to the dynamic equation on large scale (Eq. (76)). By setting parameter $\gamma = 0$, Eq. (150) reduces to the inviscid Euler equation.

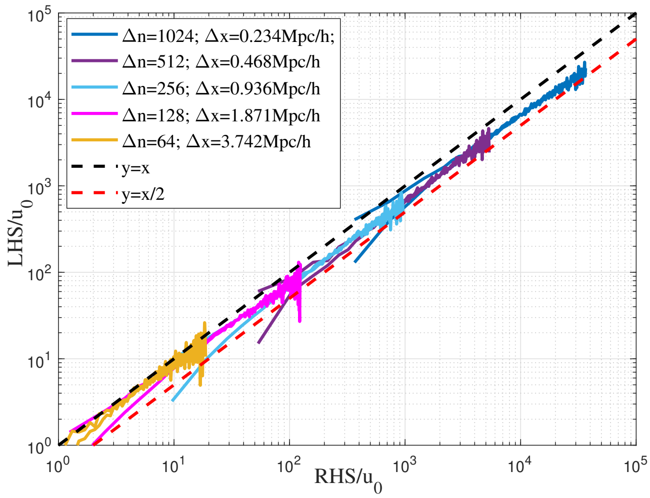

Figure 16. The value of parameter γ on different scales determined by Eq. (153) from N-body simulation at z=0. Small shift from $\gamma = 1$ on large scale (yellow line) to $\gamma = 0.5$ on small scale (blue line) can be clearly identified. The value of $\gamma = 1$ indicates the irrotational flow on large scale, while $\gamma = 0.5$ on small scale corresponds to the constant divergence flow on small scale.

The equation for vorticity field $\boldsymbol{\omega} = \nabla \times \mathbf{v}$ can be obtained by taking the curl on both sides of Eq. (148) and (150),

$$\underbrace{\frac{\partial \boldsymbol{\omega}}{\partial t} + \frac{1}{a}\nabla \times \left(\mathbf{v} \cdot \nabla \mathbf{v}\right) + H\boldsymbol{\omega}}_{LHS} = \gamma \underbrace{\frac{1}{a}\nabla \times \left[\left(\nabla \times \mathbf{v}\right) \times \mathbf{v}\right]}_{RHS}, \tag{153}$$

or

$$\frac{\partial \boldsymbol{\omega}}{\partial t} + H\boldsymbol{\omega} = \frac{1}{a}\left(\gamma - 1\right)\nabla \times \left(\mathbf{v} \cdot \nabla \mathbf{v}\right). \tag{154}$$

For $\gamma = 1$, vorticity simply decays with time and there is no source to generate vorticity on large scale. While for $\gamma < 1$, vorticity is continuously generated on small scale (see Eq. (162)). Both Equations can be used to determine the value of γ from N-body simulation.

Figure 16 plots the variation of γ with scale (the grid size Δx). The particle velocity field was projected onto grids using Cloud-in-Cell (CIC) (Hockney & Eastwood 1988) with a given grid size of Δx, or equivalently $\Delta x \cdot \Delta n = L$, where $L = 239.5Mpc/h$ is the size of simulation domain. The LHS and RHS terms in Eq. (153) were computed using the projected velocity field and plotted in Fig. 16. The slope gives the value of γ from simulation. The two dash lines for $\gamma = 1$ and $\gamma = 1/2$ are also plotted for comparison. For large grid size Δx (on large scale), γ approaches 1. While for small size Δx (on small scale), γ approaches 1/2. For the entire range of scales, $1/2 \leqslant \gamma \leqslant 1$ is expected.

7.1.2 Averaged dynamic equations for velocity and the origin of effective viscosity

The original "adhesion approximation" on large scale is a phenomenological model and a mean-field description of true dynamics. However, this model should be deeply rooted in the large-scale dynamics and kinematics and can be derived with appropriate closures between velocity fluctuation and mean velocity field (Eq. (157)).

Let's start from the time averaged equation of self-gravitating collisionless dark matter flow (Eq. (150)). By decomposing the total velocity and potential into the mean and (temporal) fluctuation,

$$\mathbf{v} = \bar{\mathbf{v}} + \mathbf{v}' \quad \text{and} \quad \phi^* = \overline{\phi^*} + \phi^{*'}, \tag{155}$$

plugging into Eq. (150) and taking the (time) average through filtering at a cutoff scale τ, we obtain an averaged dynamic equation for $\bar{\mathbf{v}}$,

$$\begin{aligned}\frac{\partial \bar{\mathbf{v}}}{\partial t} &+ \frac{1}{a}(1-\gamma)\,\bar{\mathbf{v}}\cdot\nabla\bar{\mathbf{v}} + \frac{\gamma}{2a}\nabla(\bar{\mathbf{v}}\cdot\bar{\mathbf{v}}) + H\bar{\mathbf{v}} \\ &= -\frac{1}{a}\nabla\overline{\phi^*} - \left(\frac{1-\gamma}{a}\underbrace{\overline{\mathbf{v}'\cdot\nabla\mathbf{v}'}}_{1} + \frac{\gamma}{2a}\underbrace{\overline{\nabla(\mathbf{v}'\cdot\mathbf{v}')}}_{2}\right).\end{aligned} \tag{156}$$

The eddy viscosity ν_{edd} in turbulence literature origins from term 1, i.e. $\overline{\mathbf{v}'\cdot\nabla\mathbf{v}'} = \nabla\cdot\overline{\mathbf{v}'\otimes\mathbf{v}'} = \nu_{edd}\nabla^2\bar{\mathbf{v}}$ for incompressible flow. For irrotational flow on large scale in SG-CFD, by setting $\gamma = 1$, $\nabla\overline{\phi^*} = -3Ha\bar{\mathbf{v}}/2 - a\nu\nabla^2\bar{\mathbf{v}}$ (see Eq. (152)) and comparing Eq. (156) with the dynamics of mean flow on scale τ (replacing $\nu(a)$ by $\nu_\tau(a,\tau)$ in Eq. (76), which is the effective viscosity on cutoff scale τ), the "artificial" viscosity in adhesion model originates from the velocity fluctuation (terms 2) in Eq. (156). The comparison shows

$$-\frac{1}{2a}\nabla\left(\overline{\mathbf{v}'\cdot\mathbf{v}'}\right) = (\Delta\nu)\nabla^2\bar{\mathbf{v}} = (\Delta\nu)\nabla(\nabla\cdot\bar{\mathbf{v}}), \tag{157}$$

which is the closure relating velocity fluctuation below cutoff scale τ with the mean velocity above scale τ through viscosity $\Delta\nu = \nu_\tau - \nu$. Similar to the "Reynolds stress" in turbulence (Xu 2022e), velocity fluctuation below the cutoff scale ($\mathbf{v}'$) leads to an "artificial stress" term (RHS of Eq. (157)) applied onto the dynamics for mean velocity above that cutoff scale ($\bar{\mathbf{v}}$) in averaged Eq. (156). Therefore, the effective viscosity in adhesion model has an origin from the velocity fluctuation below the cutoff scale τ.

Using Eq. (107) for relation between overdensity and divergence,

$$\begin{aligned}&\nabla\left(\overline{\mathbf{v}'\cdot\mathbf{v}'}\right) = 2a^2Hf(\Omega_m)(\Delta\nu)\nabla\bar{\delta},\\ &\text{or equivalently (after integration)}\\ &\overline{\mathbf{v}'^2} = F(t) + 2(\Delta\nu)a^2Hf(\Omega_m)\,\bar{\delta},\end{aligned} \tag{158}$$

where $F(t)$ is a function emerging after integration and $\bar{\delta}$ is the (time) average density above that cutoff scale. Equation (158) is essentially a sub-grid closure for large scale dynamics, where unresolved velocity fluctuation below a cutoff scale τ can be related to the resolved mean density at the same location through an effective viscosity ν.

The total kinetic energy (a function of time t only due to translational symmetry) can be decomposed into the kinetic energy in mean flow (resolved) and in fluctuation (unresolved),

$$\begin{aligned}\overline{\mathbf{v}^2} \equiv \overline{\mathbf{v}^2}(t) \equiv \overline{(\bar{\mathbf{v}}+\mathbf{v}')^2} &= \bar{\mathbf{v}}^2 + \overline{\mathbf{v}'^2}\\ &= \bar{\mathbf{v}}^2 + F(t) + 2(\Delta\nu)a^2Hf(\Omega_m)\,\bar{\delta},\end{aligned} \tag{159}$$

such that the kinetic energy in mean flow reads (same as Eq. (113)),

$$\bar{\mathbf{v}}^2 = \overline{\mathbf{v}^2}(t) - F(t) - 2(\Delta\nu)Ha^2f(\Omega_m)\,\bar{\delta}. \tag{160}$$

On large scale, the gravitational collapse leads to a decreasing dispersion in mean flow $\bar{\mathbf{v}}^2$. There is a continuous energy transfer from mean flow ($\bar{\mathbf{v}}^2$) to fluctuation (random motion in $\overline{\mathbf{v}'^2}$) on large scale. Combined with the energy transfer from mean flow to fluctuation on halo scale (Xu 2022e), both facilitates the continuously increasing entropy in non-equilibrium dark matter flow (Xu 2021c).

7.1.3 Equations for the evolution of vorticity and enstrophy

The vorticity field is important on small scale, as every halo has a finite spin. With identity in Eq. (73) and the identity for two arbitrary vectors **A** and **B**,

$$\nabla\times(\mathbf{A}\times\mathbf{B}) = \mathbf{A}\nabla\cdot\mathbf{B} - \mathbf{B}\nabla\cdot\mathbf{A} + \mathbf{B}\cdot\nabla\mathbf{A} - \mathbf{A}\cdot\nabla\mathbf{B}, \tag{161}$$

Eq. (154) can be transformed to (note that $\nabla\cdot\boldsymbol{\omega} = 0$):

$$\frac{\partial\boldsymbol{\omega}}{\partial t} + \frac{1-\gamma}{a}\underbrace{\mathbf{v}\cdot\nabla\boldsymbol{\omega}}_{1} + \left[1 + (1-\gamma)\frac{\theta}{Ha}\right]\underbrace{H\boldsymbol{\omega}}_{2} = \frac{1-\gamma}{a}\underbrace{\boldsymbol{\omega}\cdot\nabla\mathbf{v}}_{3}. \tag{162}$$

From identity (74), velocity field can be expressed in terms of the vorticity field for constant divergence flow,

$$\nabla^2\mathbf{v} = -\nabla\times\boldsymbol{\omega}. \tag{163}$$

For infinite domain, this can be solved by Green's function,

$$\mathbf{v}(\mathbf{x}) = -\frac{1}{4\pi}\int\frac{[\nabla\times\boldsymbol{\omega}]'}{|\mathbf{x}-\mathbf{x}'|}d\mathbf{x}', \tag{164}$$

where vorticity is a local quantity, but velocity can be non-local. The velocity field is affected by the vorticity from other locations.

Three terms in Eq. (162) represent the transport of vorticity (term 1), the decaying of vorticity due to expanding background (term 2), and the generation of vorticity (term 3) that is similar to the vortex stretching in hydrodynamic turbulence (see Xu 2021f, Eq. (1)). On large scale, $\gamma \approx 1$ and the dominant mode is the decaying of vorticity, while vorticity is strongly generated with $\gamma \to 1/2$ on small scale. For comparison, the vorticity equation for incompressible flow is

$$\frac{\partial\boldsymbol{\omega}}{\partial t} + \mathbf{v}\cdot\nabla\boldsymbol{\omega} = \boldsymbol{\omega}\cdot\nabla\mathbf{v} + \nu\nabla^2\boldsymbol{\omega}, \tag{165}$$

where ν is the molecular viscosity leading to the destruction of vorticity. Finally, the evolution of enstrophy can be obtained by the scalar product of Eq. (162) with vorticity vector $\boldsymbol{\omega}$,

$$\begin{aligned}\frac{\partial\omega^2/2}{\partial t} &+ \frac{1-\gamma}{a}\underbrace{\mathbf{v}\cdot\nabla\frac{\omega^2}{2}}_{1} + \left[1 + (1-\gamma)\frac{\theta}{Ha}\right]\underbrace{H\omega^2}_{2}\\ &= \frac{1-\gamma}{a}\underbrace{\boldsymbol{\omega}\cdot(\boldsymbol{\omega}\cdot\nabla\mathbf{v})}_{3},\end{aligned} \tag{166}$$

where the enstrophy is generated on the small scale (term 3), transported (term 1) and decaying on large scale (term 2).

7.1.4 Dynamic equations for the evolution of energy

By taking scalar product **v** with both sides of Eq. (148) and using the fact that $\mathbf{v}\cdot(\nabla\times\mathbf{v})\times\mathbf{v} = 0$, the evolution of kinetic energy reads

$$\frac{\partial\mathbf{v}^2/2}{\partial t} + \frac{1}{a}\mathbf{v}\cdot[\mathbf{v}\cdot\nabla(\mathbf{v})] + H\mathbf{v}^2 = -\frac{1}{a}\mathbf{v}\cdot\nabla\phi^*. \tag{167}$$

Using identity (73) and $\mathbf{v}\cdot(\nabla\times\mathbf{v})\times\mathbf{v} = 0$, Eq. (167) becomes

$$\frac{\partial\mathbf{v}^2/2}{\partial t} = -\frac{1}{a}\nabla\cdot\left[\left(\frac{1}{2}\mathbf{v}^2+\phi^*\right)\mathbf{v}\right] - H\mathbf{v}^2 + \frac{1}{a}\left(\frac{1}{2}\mathbf{v}^2+\phi^*\right)\nabla\cdot\mathbf{v}. \tag{168}$$

Integrating Eq. (168) over a control volume V (for example the volume of a halo) and using divergence theorem,

$$\frac{\partial K}{\partial t} = -\frac{1}{a}\oint_S E\mathbf{v}\cdot d\mathbf{S} - 2HK + \frac{1}{a}\int_V E(\nabla\cdot\mathbf{v})\,dV, \tag{169}$$

where the specific kinetic energy K of entire volume and the total energy E at a given location are defined as

$$K=\int_V \frac{1}{2}\mathbf{v}\cdot\mathbf{v}dV \quad \text{and} \quad E=\frac{1}{2}\mathbf{v}^2+\phi^*. \tag{170}$$

For system with $E=0$ on the surface of control volume, the surface term vanishes in Eq. (169). Introducing virial theorem between the total kinetic and potential energy with a virial ratio β,

$$\int_V \left(2\mathbf{v}^2+\beta\phi^*\right)dV=0, \tag{171}$$

the time variation of total kinetic energy in control volume is,

$$\frac{\partial \ln K}{\partial \ln a}=-\frac{\theta}{aH}\left(\frac{4}{\beta}-1\right)-2. \tag{172}$$

By taking the divergence on both sides of Eq. (148), we have

$$\frac{\partial\theta}{\partial t}+\frac{1}{2a}\nabla^2(\mathbf{v}\cdot\mathbf{v})+H\theta=-\frac{1}{a}\nabla^2\phi^*+\frac{\gamma-1}{a}\nabla\cdot[(\nabla\times\mathbf{v})\times\mathbf{v}]. \tag{173}$$

With the identity in Eq. (74) and identity

$$\nabla\cdot(\mathbf{A}\times\mathbf{B})=(\nabla\times\mathbf{A})\cdot\mathbf{B}-\mathbf{A}\cdot(\nabla\times\mathbf{B}), \tag{174}$$

the equation for total energy E can be obtained,

$$\begin{aligned}\nabla^2\left(\frac{1}{2}\mathbf{v}\cdot\mathbf{v}+\phi^*\right)+Ha\theta\left(1+\frac{\partial\ln\theta}{\partial\ln a}\right)\\ =(1-\gamma)\left(\left[\mathbf{v}\cdot\left(\nabla^2\mathbf{v}-\nabla\theta\right)+\boldsymbol{\omega}\cdot\boldsymbol{\omega}\right]\right).\end{aligned} \tag{175}$$

On large scale, $\gamma=1$ and $\theta=-aHf(\Omega_m)\delta\propto a^{1/2}$ (Eq. (107)),

$$\nabla^2\left(\frac{1}{2}\mathbf{v}\cdot\mathbf{v}+\phi^*\right)=f(\Omega_m)\nabla^2\phi=\frac{3}{2}a^2H^2f(\Omega_m)\delta, \tag{176}$$

where ϕ is the (peculiar) gravitational potential. The potential well forms from increasing δ due to gravitational collapse. On small scale with constant divergence and $\theta\propto a^{-1/2}$,

$$\nabla^2\left(\frac{1}{2}\mathbf{v}\cdot\mathbf{v}+\phi^*\right)=-\frac{1}{2}Ha\theta+(1-\gamma)\left(\mathbf{v}\cdot\nabla^2\mathbf{v}+\boldsymbol{\omega}\cdot\boldsymbol{\omega}\right), \tag{177}$$

where the local vorticity will affect the depth of potential well.

7.2 Dynamic relations from dynamics on small scale

In this section, we are ready to develop dynamic relations on small scale. Starting from the index notation of dynamic Eq. (151) at two different locations $\mathbf{x}$ and $\mathbf{x}'$,

$$\begin{aligned}\frac{\partial v_i}{\partial t}+\frac{1-\gamma}{a}\frac{\partial(v_iv_k)}{\partial x_k}+\frac{\gamma}{2a}\frac{\partial(v_kv_k)}{\partial x_i}\\ +\left[1-\frac{(1-\gamma)}{aH}\theta\right]Hv_i=-\frac{1}{a}\frac{\partial\phi^*}{\partial x_i},\end{aligned} \tag{178}$$

$$\begin{aligned}\frac{\partial v_j'}{\partial t}+\frac{1-\gamma}{a}\frac{\partial\left(v_j'v_k'\right)}{\partial x_k'}+\frac{\gamma}{2a}\frac{\partial\left(v_k'v_k'\right)}{\partial x_j'}\\ +\left[1-\frac{(1-\gamma)}{aH}\theta\right]Hv_j'=-\frac{1}{a}\frac{\partial\phi^{*'}}{\partial x_j'},\end{aligned} \tag{179}$$

multiplying v_j' and v_i to both sides of two equations, adding them together, and taking average at a given scale r leads to

$$\begin{aligned}&\frac{\partial\left\langle v_iv_j'\right\rangle}{\partial t}+\frac{1-\gamma}{a}\left(\frac{\partial\left\langle v_iv_kv_j'\right\rangle}{\partial x_k}+\frac{\partial\left\langle v_j'v_k'v_i\right\rangle}{\partial x_k'}\right)\\ &+\frac{\gamma}{2a}\left(\frac{\partial\left\langle v_kv_kv_j'\right\rangle}{\partial x_i}+\frac{\partial\left\langle v_k'v_k'v_i\right\rangle}{\partial x_j'}\right)\\ &+2\left[1-\frac{(1-\gamma)}{aH}\theta\right]H\left\langle v_iv_j'\right\rangle=-\frac{1}{a}\left(\frac{\partial\left\langle\phi^*v_j'\right\rangle}{\partial x_i}+\frac{\partial\left\langle\phi^{*'}v_i\right\rangle}{\partial x_j'}\right),\end{aligned} \tag{180}$$

or in terms of the second and third order velocity correlation tensors (see definition in Eq. (1)),

$$\begin{aligned}&\frac{\partial Q_{ij}}{\partial t}+2\left[1-\frac{(1-\gamma)}{aH}\theta\right]HQ_{ij}\\ &=\frac{2-2\gamma}{a}\frac{\partial Q_{ikj}}{\partial r_k}+\frac{\gamma}{a}\frac{\partial Q_{kkj}}{\partial r_i}-\frac{1}{a}\left[\frac{\partial\left\langle\phi^*v_j'\right\rangle}{\partial x_i}+\frac{\partial\left\langle\phi^{*'}v_i\right\rangle}{\partial x_j'}\right].\end{aligned} \tag{181}$$

Multiplying both sides by δ_{ij}, using Eqs. (15) and (84) for third order correlations with $R_3\equiv R_{(3,1)}$ and $R_{31}\equiv L_{(3,2)}$, and using the fact that the first order correlation tensor for constant divergence flow (see Xu 2022f, Eq. (9)) satisfying,

$$\frac{\partial\left\langle\phi^*v_j'\right\rangle}{\partial x_j}=-\frac{\partial\left\langle\phi^*v_j'\right\rangle}{\partial r_j}=-\theta\left\langle\phi^*\right\rangle, \tag{182}$$

evolution of second order correlation on small scale finally reads

$$\begin{aligned}&\frac{\partial R_{(2,1)}}{\partial t}+2\left[1-\frac{(1-\gamma)}{aH}\theta\right]HR_{(2,1)}\\ &=\frac{1}{ar^2}\left[\frac{\partial}{\partial r}\left(r^2\left[(2-2\gamma)R_{(3,1)}+\gamma L_{(3,2)}\right]\right)\right]+\frac{2}{a}\theta\left\langle\phi^*\right\rangle,\end{aligned} \tag{183}$$

where third order correlation functions are (Eqs. (15) and (84))

$$\frac{\partial Q_{iki}}{\partial r_k}=\frac{1}{r^2}\frac{\partial}{\partial r}\left(r^2R_{(3,1)}\right),\quad \frac{\partial Q_{kkj}}{\partial r_j}=\frac{1}{r^2}\frac{\partial}{\partial r}\left(r^2L_{(3,2)}\right). \tag{184}$$

Equation (183) provides a dynamic relation between second and third order correlation functions (similar to Eq. (81) on large scale), which can be integrated and equivalently transformed to,

$$\begin{aligned}&\frac{-\left\langle\phi^*\right\rangle}{u^2}=\frac{3}{2\theta ru^2}\left[(2-2\gamma)R_{(3,1)}+\gamma L_{(3,2)}\right]\\ &+\left[(1-\gamma)\frac{2\theta}{aH}-2-\frac{\partial\ln R_{(2,1)}}{\partial\ln a}\right]\frac{3Ha}{2u^2\theta r^3}\int_0^r R_{(2,1)}(y)\,y^2dy.\end{aligned} \tag{185}$$

On small scale, the correlation function $R_{(2,1)}$ can be modeled as (see Xu 2022f, Eq. (139)),

$$R_{(2,1)}=u^2\left[3-(3+n)\left(\frac{r}{r_1}\right)^n\right] \quad \text{and} \quad \frac{\partial\ln R_{(2,1)}}{\partial\ln a}=\frac{3}{2}, \tag{186}$$

with $u^2\sim t$, where u^2 is the one-dimensional velocity dispersion of entire system and $n\approx 1/4$. The correlation function $R_{(2,1)}\propto a$ on large scale and $R_{(2,1)}\propto a^{3/2}$ on small scale.

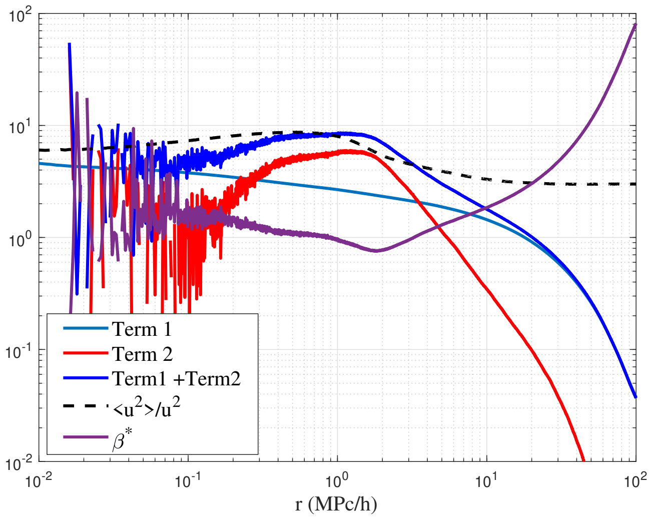

Figure 17. The variation of different terms in Eq. (187) with scale r at z=0. On small scale, term 1 approaches 5 and term2 approaches 1. The sum of term1 and term2 approaches the velocity dispersion $\left\langle u^2\right\rangle/u^2$. The variation of virial coefficient β^* with scale r (slightly decreasing with r) is also presented with $\left\langle u^2\right\rangle/u^2$ directly obtained from simulation and Eq. (187).

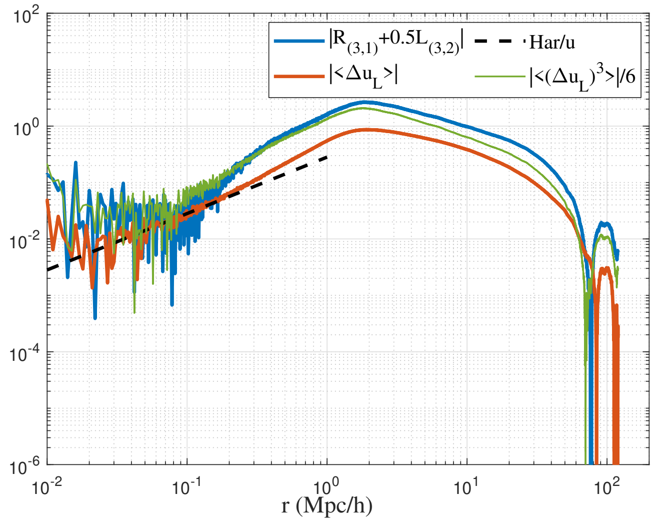

Figure 18. The variation of correlation function $R_{(3,1)}+L_{(3,2)}/2$ at $z=0$ (normalized by u_0^3), the pairwise velocity (first order longitudinal structure function) $\langle\Delta u_L\rangle$ (normalized by u_0), and the third order longitudinal structure function $\langle(\Delta u_L)^3\rangle$ (normalized by u_0^3) with scale r (from Eqs. (188) and (191)). All functions are normalized and $\langle(\Delta u_L)^3\rangle = 8\varepsilon_u ar/3$.

On small scale, we expect $\gamma = 1/2$ and $\theta = -3Ha/2$, and relation $\langle u^2\rangle + \beta^*\langle\phi^*\rangle = 0$, Eq. (185) reduces to

$$\frac{-\langle\phi^*\rangle}{u^2} = \frac{\langle u^2\rangle}{\beta^* u^2} = \underbrace{\frac{5}{u^2 r^3}\int_0^r R_{(2,1)}(y)\,y^2 dy}_{1} \underbrace{-\frac{1}{Haru^2}\left(R_{(3,1)}+\frac{1}{2}L_{(3,2)}\right)}_{2}, \tag{187}$$

where β^* is a virial ratio on scale r.

To validate Eq. (187), different terms were directly obtained from N-body simulation and plotted in Fig. 17. The sum of terms 1 and 2 on the RHS of Eq. (187) approaches LHS on small scale. The variation of β^* with scale r (slightly decreasing with r) is also presented with $\left\langle u^2\right\rangle/u^2$ directly obtained from simulation.

For $r \to 0$, we have $\lim_{r\to 0} R_{(2,1)} = \lim_{r\to 0}\langle\mathbf{u}\cdot\mathbf{u}'\rangle = 3u^2$ and $\lim_{r\to 0}\langle u^2\rangle = \lim_{r\to 0}\langle\mathbf{u}\cdot\mathbf{u}\rangle = 6u^2$, where $\langle u^2\rangle \approx 6u^2$ on small scale (see Xu 2022h, Fig. 20) and $\beta^* \approx 1$, term 1 on RHS of Eq. (187) approaches 5 such that term 2 becomes

$$\left(R_{(3,1)}+\frac{1}{2}L_{(3,2)}\right) = -Hau^2 r = \langle\Delta u_L\rangle u^2 = \frac{4}{9}\varepsilon_u ar, \tag{188}$$

where the rate of kinetic energy cascade ε_u is negative (inverse energy cascade) and relatively a constant of time,

$$\varepsilon_u = -\frac{3}{2}\frac{\partial u^2}{\partial t} \approx -\frac{3}{2}\frac{u^2}{t} = -\frac{3}{2}\frac{u_0^2}{t_0} \approx -4.6\times 10^{-7} m^2/s^3. \tag{189}$$

The velocity dispersion at present epoch is about $u_0 \approx 354.61 km/s$ in the current model. Since the third moment of pairwise velocity (third order structure function in Eq. (38)) satisfies (from generalized stable clustering hypothesis, GSCH in Eq. (42)),

$$\left\langle(\Delta u_L)^3\right\rangle = 3\left\langle(\Delta u_L)^2\right\rangle\langle\Delta u_L\rangle, \tag{190}$$

and $\lim_{r\to 0}\left\langle(\Delta u_L)^2\right\rangle \approx 2u^2$ (see Xu 2022h, Fig. 21), we may write

$$\left(R_{(3,1)}+\frac{1}{2}L_{(3,2)}\right) = \frac{1}{6}\left\langle(\Delta u_L)^3\right\rangle = \langle\Delta u_L\rangle u^2 = \frac{4}{9}\varepsilon_u ar, \tag{191}$$

where the third moment of pairwise velocity determines the rate of energy production on the smallest scale, i.e.

$$\left\langle(\Delta u_L)^3\right\rangle = \frac{8}{3}\varepsilon_u ar \quad\text{or}\quad \varepsilon_u = \frac{3}{8}\frac{\left\langle(\Delta u_L)^3\right\rangle}{ar}. \tag{192}$$

Figure 18 presents the relevant correlation and structure functions in Eqs. (188) and (191). On small scale, all these functions can be related to the rate of energy cascade ε_u.

8 CONCLUSIONS

Much more complicated than incompressible flow, the self-gravitating collisionless dark matter flow (SG-CFD) is of constant divergence on small scale and irrotational on large scale. To understand the nature of flow across entire range of scales, fundamental kinematic and dynamic relations among statistical measures of different order need to be developed for different types of flow.

By extending the two-point second order statistics to high order, we present the third order statistical measures and associated kinematic relations for different types of flow. In principle, the incompressible and constant divergence flow share the same kinematic relations for even order correlations, while they can be different for odd order correlations (Eq. (56)). For third order velocity correlation tensor $Q_{ijk}(r)$, four scalar correlation functions (total correlations R_3 and R_{31}, longitudinal correlation L_3, and transverse correlation T_3) can be obtained by contraction of indices from $Q_{ijk}(r)$ (Eqs. (6)-(9)). Kinematic relations are developed for incompressible flow (Eqs. (26) and (27)), constant divergence flow (Eqs. (31) and (33)), and irrotational flow (Eq. (37)). Correlation functions from N-body simulation are presented in Figs. 3 and 4 for third and fourth order, respectively.

To formulate kinematic relations of any order, a compact derivation is presented involving high order tensor and vector calculus. This is a challenging task (see Appendix A). Starting from reformulating the kinematic relations of second and third order, general kinematic relations of any order are developed, i.e. Eqs. (53)-(55) for incompressible flow, Eq. (62) for constant divergence on small scale, and Eqs. (63)-(65) for irrotational flow on large scale. To validate these relations by N-body simulation, the original differential equations are transformed to integral form (Eqs. (67) to (69)). Results are presented in Figs. 6 and 7 with good agreement.

The dynamic relations between correlation functions of different orders can only be determined from the dynamic equation of velocity evolution on relevant scales. On large scale, the Zeldovich and adhesion approximations govern the dynamics of velocity (Eq. (70)). Third order correlations are related to second order velocity/density correlations and mean pairwise velocity ($L_{(3,2)} \propto -\nu\langle\Delta u_L\rangle$) through an effective viscosity $\nu(a)$ (Eqs. (88), (91), and (94)). The negative viscosity $\nu(a) \propto -ur_2 \propto a^{1/2}$ originates from the velocity fluctuation (Eq. (158)) and can be determined by the rate of energy production (Eq. (97) and Fig. 12).

Redshift dependence of correlations functions on any order are obtained as $L_{(q+1,q)} \propto a^{(q+3)/2}$ and $R_{(q,q-1)} \propto a^{q/2}$ for even q (Eqs. (100)-(102) and Figs. 8-12). The divergence can be determined by the mean pairwise velocity (Eq. (108)). Mean overdensity on a given scale r is proportional to the density correlation $f(\Omega_m)\langle\delta\rangle \approx \langle\delta\delta^{'}\rangle$ (Eq. (110) and Fig. 13)). A reduced velocity dispersion is also proportional to density correlation, i.e. $\langle u^2\rangle/(3u^2) - 1 \propto \langle\delta\delta^{'}\rangle$ (Eq. (113) and Fig. 13)). Finally, both exponential velocity correlations on large scale and the "one-fourth" law for correlations on small scale are direct results of combined dynamics and kinematic relations (Eqs. (128), (129), and (123)).

On small scale, self-closed equation for velocity evolution is developed to derive dynamic relations. We decompose total velocity into the velocity from motion in halos and from the motion of halos (Eq. (132)). Based on solutions for virialized rotating halos, the self-closed dynamic equation includes an additional term to reflect the effect of local vorticity (term 1 in Eq. (148)) that is controlled by a parameter γ. From large to small scales, γ gradually changes from 1 to 1/2 (Fig. 16). The effective viscosity on large scale origins from the velocity fluctuations below the cutoff scale for filtering (Eq. (156)). The vorticity, enstrophy, and energy evolution are all derived from the self-closed dynamic equation (Eqs. (162), (166), (168), and (175)). Finally, the dynamic relation is derived to relate second and third order correlations in Eq. (183). The same relation in integral form (Eqs. (185) and (187)) can be directly validated by N-body simulation (Fig. 17). Third order correlations are related to the energy production rate ε_u (Eq. (191) and Fig. 18) and third moment of pairwise velocity $\langle(\Delta u_L)^3\rangle = 8\varepsilon_u ar/3$ (Eq. (192)).

DATA AVAILABILITY

Two datasets underlying this article, i.e. a halo-based and correlation-based statistics of dark matter flow, are available on Zenodo (Xu 2022a,b), along with the accompanying presentation slides "A comparative study of dark matter flow & hydrodynamic turbulence and its applications" (Xu 2022c). All data files are also available on GitHub (Xu 2022d).

REFERENCES

Angulo R. E., Springel V., White S. D. M., Jenkins A., Baugh C. M., Frenk C. S., 2012, Monthly Notices of the Royal Astronomical Society, 426, 2046

Batchelor G. K., 1953, The Theory of Homogeneous Turbulence. Cambridge University Press, Cambridge, UK

Borgani S., da Costa L. N., Zehavi I., Giovanelli R., Haynes A. P., Freudling W., Wegner G., Salzer J. J., 2000, Astronomical Journal, 119, 102

Buchert T., Dominguez A., 2005, Astronomy & Astrophysics, 438, 443

Colberg J. M., White S. D. M., Jenkins A., Pearce F. R., 1999, Monthly Notices of the Royal Astronomical Society, 308, 593

Davis M., Peebles P. J. E., 1977, Astrophysical Journal Supplement Series, 34, 425

Efstathiou G., Davis M., Frenk C. S., White S. D. M., 1985, Astrophysical Journal Supplement Series, 57, 241

Ferreira P. G., Juszkiewicz R., Feldman H. A., Davis M., Jaffe A. H., 1999, Astrophysical Journal, 515, L1

Frenk C. S., et al., 2000, arXiv:astro-ph/0007362v1

Gorski K., 1988, Astrophysical Journal, 332, L7

Gorski K. M., Davis M., Strauss M. A., White S. D. M., Yahil A., 1989, Astrophysical Journal, 344, 1

Gurbatov S. N., Saichev A. I., Shandarin S. F., 1989, Monthly Notices of the Royal Astronomical Society, 236, 385

Hellwing W. A., Barreira A., Frenk C. S., Li B. J., Cole S., 2014, Physical Review Letters, 112

Hockney R. W., Eastwood J. W., 1988, Computer Simulation Using Particles. Taylor & Francis, Bristol, PA, USA

Jenkins A., et al., 1998, Astrophysical Journal, 499, 20

Juszkiewicz R., Ferreira P. G., Feldman H. A., Jaffe A. H., Davis M., 2000, Science, 287, 109

Kitaura F. S., Ata M., Angulo R. E., Chuang C. H., Rodriguez-Torres S., Monteagudo C. H., Prada F., Yepes G., 2016, Monthly Notices of the Royal Astronomical Society, 457, L113

Kolmogoroff A., 1941a, Comptes Rendus De L Academie Des Sciences De L Urss, 30, 301

Kolmogoroff A. N., 1941b, Comptes Rendus De L Academie Des Sciences De L Urss, 32, 16

Ma Y. Z., Li M., He P., 2015, Astronomy & Astrophysics, 583

Mo H., van den Bosch F., White S., 2010, Galaxy formation and evolution. Cambridge University Press, Cambridge

Peebles P. J. E., Melott A. L., Holmes M. R., Jiang L. R., 1989, Astrophysical Journal, 345, 108

Pueblas S., Scoccimarro R., 2009, Physical Review D, 80, 043504

Sheth R. K., Mo H. J., Tormen G., 2001, Monthly Notices of the Royal Astronomical Society, 323, 1

Springel V., 2005, Monthly Notices of the Royal Astronomical Society, 364, 1105

Taylor G. I., 1932, Proceedings of the Royal Society of London Series a-Containing Papers of a Mathematical and Physical Character, 135, 685

Taylor G. I., 1935, Proceedings of the royal society A, 151, 421

Xu Z., 2021a, arXiv e-prints, p. arXiv:2109.09985

Xu Z., 2021b, arXiv e-prints, p. arXiv:2109.12244

Xu Z., 2021c, arXiv e-prints, p. arXiv:2110.03126

Xu Z., 2021d, arXiv e-prints, p. arXiv:2110.05784

Xu Z., 2021e, arXiv e-prints, p. arXiv:2110.09676

Xu Z., 2021f, arXiv e-prints, p. arXiv:2110.13885

Xu Z., 2022c, A comparative study of dark matter flow & hydrodynamic turbulence and its applications, doi:10.5281/zenodo.6569901, `http://dx.doi.org/10.5281/zenodo.6569901`

Xu Z., 2022d, Dark matter flow dataset, doi:10.5281/zenodo.6586212, `https://github.com/ZhijieXu2022/dark_matter_flow_dataset`

Xu Z., 2022a, Dark matter flow dataset Part I: Halo-based statistics from cosmological N-body simulation, doi:10.5281/zenodo.6541230, `http://dx.doi.org/10.5281/zenodo.6541230`

Xu Z., 2022b, Dark matter flow dataset Part II: Correlation-based statistics from cosmological N-body simulation, doi:10.5281/zenodo.6569898,

http://dx.doi.org/10.5281/zenodo.6569898
Xu Z., 2022e, arXiv e-prints, p. arXiv:2201.12665
Xu Z., 2022f, arXiv e-prints, p. arXiv:2202.00910
Xu Z., 2022g, arXiv e-prints, p. arXiv:2202.04054
Xu Z., 2022h, arXiv e-prints, p. arXiv:2202.06515
Xu Z., 2022i, arXiv e-prints, p. arXiv:2202.07240
Xu Z., 2022j, arXiv e-prints, p. arXiv:2203.05606
Xu Z., 2022k, arXiv e-prints, p. arXiv:2203.06899
de Karman T., Howarth L., 1938, Proceedings of the Royal Society of London Series a-Mathematical and Physical Sciences, 164, 0192

APPENDIX A: KINEMATIC RELATIONS FOR VELOCITY CORRELATIONS OF ARBITRARY ORDER

In this Appendix, a compact derivation for kinematic relations of arbitrary order is presented for incompressible, constant divergence, and irrotational flow.

A1 Introduction to some general identities

Let's first introduce some identities, which are the generalization of identities in Eq. (25),

$$(\hat{r}_i)_{,j} = \frac{\partial \hat{r}_i}{\partial r_j} = \frac{1}{r}\left(\delta_{ij} - \hat{r}_i\hat{r}_j\right) = (\hat{r}_j)_{,i}\,, \tag{A1}$$

$$\left(\hat{r}_i\hat{r}_j\right)_{,k} = \frac{1}{r}\left(\hat{r}_i\delta_{jk} + \hat{r}_j\delta_{ik} - 2\hat{r}_i\hat{r}_j\hat{r}_k\right), \tag{A2}$$

$$\left(\hat{r}_i\hat{r}_j\hat{r}_k\right)_{,l} = \frac{1}{r}\left(\hat{r}_i\hat{r}_j\delta_{kl} + \hat{r}_i\hat{r}_k\delta_{jl} + \hat{r}_j\hat{r}_k\delta_{il} - 3\hat{r}_i\hat{r}_j\hat{r}_k\hat{r}_l\right), \tag{A3}$$

$$\begin{aligned}\left(\hat{r}_i\hat{r}_j\hat{r}_k\hat{r}_l\right)_{,m} = \frac{1}{r}&\left(\hat{r}_i\hat{r}_j\hat{r}_l\delta_{km} + \hat{r}_i\hat{r}_k\hat{r}_l\delta_{jm}\right.\\ &\left.+\hat{r}_i\hat{r}_j\hat{r}_k\delta_{lm} + \hat{r}_j\hat{r}_k\hat{r}_l\delta_{im} - 4\hat{r}_i\hat{r}_j\hat{r}_k\hat{r}_l\hat{r}_m\right),\end{aligned} \tag{A4}$$

$$(\hat{r}_i)_{,j}\,\hat{r}_j = 0,\ \left(\hat{r}_i\hat{r}_j\right)_{,k}\hat{r}_k = 0,\ \left(\hat{r}_i\hat{r}_j\hat{r}_k\right)_{,l}\hat{r}_l = 0, \tag{A5}$$

$$(\hat{r}_i)_{,i} = \frac{2}{r},\ \left(\hat{r}_i\hat{r}_j\right)_{,j} = \frac{2}{r}\hat{r}_i,\ \left(\hat{r}_i\hat{r}_j\hat{r}_k\right)_{,k} = \frac{2}{r}\hat{r}_i\hat{r}_j, \tag{A6}$$

$$(r_i)_{,j} = \delta_{ij},\ \left(\hat{r}_i r_j\right)_{,j} = 3\hat{r}_i,\ \left(\hat{r}_i\hat{r}_j r_k\right)_{,k} = 3\hat{r}_i\hat{r}_j. \tag{A7}$$

In the following, we first reformulate kinematic relations in a more general but compact way for second and third correlation functions to get familiar with the general idea and tensor notations, followed by the generalization to arbitrary orders.

A2 Reformulating second order kinematic relations

The starting point of new formulation is definitions of correlation tensor Q_{ij} and associated correlation functions R_2, L_2, and T_2,

$$\begin{aligned}&Q_{ij}(r) = \left\langle u_i u_j^{'}\right\rangle, \quad R_2 = \left\langle u_i u_i^{'}\right\rangle,\\ &L_2 = \left\langle u_L u_L^{'}\right\rangle, \quad \text{and} \quad R_2 = L_2 + 2T_2.\end{aligned} \tag{A8}$$

With isotropic homogeneous second order correlation tensor defined as (see Xu 2022f, Eq. (10)),

$$Q_{ij}(\mathbf{r}) = Q_{ij}(r) = A_2(r)\, r_i r_j + B_2(r)\,\delta_{ij}, \tag{A9}$$

we should have an identity valid for any type of flow,

$$\begin{aligned}Q_{ij}\hat{r}_i\left(\delta_{jk} - \hat{r}_j\hat{r}_k\right) &= \left\langle u_L u_j^{'}\right\rangle\left(\delta_{jk} - \hat{r}_j\hat{r}_k\right)\\ &= \left\langle u_L u_k^{'}\right\rangle - \left\langle u_L u_L^{'}\hat{r}_k\right\rangle = 0.\end{aligned} \tag{A10}$$

This is an important identity that we will repeatedly use.

A2.1 Kinematic relations for incompressible flow

Using identity in Eq. (A1), the relation $u_L = u_i\hat{r}_i$, and the product rule of differentiation,

$$\begin{aligned}Q_{ij,j}\hat{r}_i = \left\langle u_i u_j^{'}\right\rangle_{,j}\hat{r}_i &= \left\langle u_i\hat{r}_i u_j^{'}\right\rangle_{,j} - \left\langle u_i u_j^{'}\right\rangle(\hat{r}_i)_j\\ &= \left\langle u_L u_j^{'}\right\rangle_{,j} - \frac{1}{r}\left\langle u_i u_j^{'}\right\rangle\left(\delta_{ij} - \hat{r}_i\hat{r}_j\right).\end{aligned} \tag{A11}$$

By using identity in Eq. (A10), Eq. (A11) can be further written as

$$\begin{aligned}&Q_{ij,j}\hat{r}_i = \left\langle u_L u_L^{'}\hat{r}_j\right\rangle_{,j} - \frac{1}{r}\left\langle u_i u_j^{'}\right\rangle\left(\delta_{ij} - \hat{r}_i\hat{r}_j\right)\\ &= \left\langle u_L u_L^{'}\right\rangle_{,j}\hat{r}_j + \left\langle u_L u_L^{'}\right\rangle(\hat{r}_j)_{,j} - \frac{1}{r}\left\langle u_i u_j^{'}\right\rangle\left(\delta_{ij} - \hat{r}_i\hat{r}_j\right).\end{aligned} \tag{A12}$$

For incompressible flow, $Q_{ij,j} = 0$. From Eq. (A12) and identity (A6), kinematic relations between second order correlation functions can be obtained in a very simple and compact way,

$$\begin{aligned}&2T_2 = \frac{1}{r}\left(r^2 L_2\right)_{,r},\ R_2 = \frac{1}{r^2}\left(r^3 L_2\right)_{,r},\\ &\text{and}\\ &\left(r^2 L_2\right)_{,r} = r\left(R_2 - L_2\right),\end{aligned} \tag{A13}$$

which are exact the same as our previous result (see Xu 2022f, Eq. (39)). Here the relation

$$\left\langle u_L u_L^{'}\right\rangle_{,j}\hat{r}_j = \left\langle u_L u_L^{'}\right\rangle_{,r}\hat{r}_j\hat{r}_j = \left\langle u_L u_L^{'}\right\rangle_{,r} \tag{A14}$$

is applied to Eq. (A12) for results in Eq. (A13).

A2.2 Kinematics relations for constant divergence flow on small scale

For even order correlation functions, kinematic relations for constant divergence flow should be the same as those for incompressible flow, i.e. Eq. (A13) is still valid.

A2.3 Kinematic relations for irrotational flow on large scale

The starting point to formulate kinematic relations for irrotational flow is the identity,

$$\begin{aligned}Q_{ij,k}\varepsilon_{mik}\varepsilon_{mjn}\hat{r}_n &= Q_{ij,k}\left(\delta_{ij}\delta_{kn} - \delta_{in}\delta_{jk}\right)\hat{r}_n\\ &= Q_{ij,k}\left(\hat{r}_k\delta_{ij} - \hat{r}_i\delta_{jk}\right),\end{aligned} \tag{A15}$$

where ε_{ijk} is the Levi-Civita symbol and $\hat{r}_n = \mathbf{r}/|\mathbf{r}|$ is a unit vector. With curl free condition $Q_{ij,k}\varepsilon_{mik} = 0$ and the product rule of differentiation, Eq. (A15) becomes

$$\begin{aligned}Q_{ij,k}\left(\hat{r}_k\delta_{ij} - \hat{r}_i\delta_{jk}\right) &= \left\langle u_i u_i^{'}\right\rangle_{,k}\hat{r}_k - \left\langle u_i u_j^{'}\right\rangle_{,j}\hat{r}_i\\ &= \left\langle u_i u_i^{'}\right\rangle_{,k}\hat{r}_k - \left\langle u_i u_j^{'}\hat{r}_i\right\rangle_{,j} + \left\langle u_i u_j^{'}\right\rangle(\hat{r}_i)_{,j} = 0.\end{aligned} \tag{A16}$$

With identity in Eq. (A1), $u_L = u_i\hat{r}_i$, and the help of Eq. (A10),

$$\begin{aligned}&\left\langle u_i u_i'\right\rangle_{,r} - \left\langle u_L u_j'\right\rangle_{,j} + \frac{1}{r}\left\langle u_i u_j'\right\rangle\left(\delta_{ij} - \hat{r}_i\hat{r}_j\right)\\&= \left\langle u_i u_i'\right\rangle_{,r} - \left\langle u_L u_L'\hat{r}_j\right\rangle_{,j} + \frac{1}{r}\left\langle u_i u_j'\right\rangle\left(\delta_{ij} - \hat{r}_i\hat{r}_j\right) = 0.\end{aligned} \tag{A17}$$

Using the product rule of differentiation, Eq. (A17) leads to

$$\begin{aligned}&\left\langle u_i u_i'\right\rangle_{,r} - \left\langle u_L u_L'\right\rangle_{,j}\hat{r}_j - \left\langle u_L u_L'\right\rangle\left(\hat{r}_j\right)_{,j}\\&\qquad + \frac{1}{r}\left\langle u_i u_j'\right\rangle\left(\delta_{ij} - \hat{r}_i\hat{r}_j\right) = 0.\end{aligned} \tag{A18}$$

Finally for irrotational flow, with $R_2 = L_2 + 2T_2$ and identity (A6), Eq. (A18) leads to the relations

$$\left(R_2 r\right)_{,r} = \frac{1}{r^2}\left(r^3 L_2\right)_{,r}, R_2 = \frac{1}{r^2}\left(r^3 T_2\right)_{,r}, L_2 = \left(rT_2\right)_{,r}, \tag{A19}$$

which are the same as previous result (see Xu 2022f, Eq. (47)), but obtained in a much simpler and more compact way.

A3 Reformulating third order kinematic relations

Kinematic relations for third order correlations can be derived in a similar way. Starting from the definitions of third order correlation tensor and correlation functions

$$\begin{aligned}&Q_{ijk}(r) = \left\langle u_i u_j u_k'\right\rangle, \quad R_3 = \left\langle u_L u_i u_i'\right\rangle,\\&R_{31} = \left\langle u_i u_i u_L'\right\rangle, \quad L_3 = \left\langle u_L^2 u_L'\right\rangle, \quad R_3 = L_3 + 2T_3,\end{aligned} \tag{A20}$$

we can easily verify identities (similar to Eq. (A10))

$$Q_{ijk}\hat{r}_i\hat{r}_j\left(\delta_{kl} - \hat{r}_k\hat{r}_l\right) = \left\langle u_L^2 u_l'\right\rangle - \left\langle u_L^2 u_L'\hat{r}_l\right\rangle = 0, \tag{A21}$$

$$Q_{ijk}\hat{r}_j\hat{r}_k\left(\delta_{il} - \hat{r}_i\hat{r}_l\right) = \left\langle u_l u_L u_L'\right\rangle - \left\langle u_L^2 u_L'\hat{r}_l\right\rangle = 0, \tag{A22}$$

$$Q_{ijk}\delta_{ij}\left(\delta_{kl} - \hat{r}_k\hat{r}_l\right) = \left\langle u_i u_i u_l'\right\rangle - \left\langle u_i u_i u_L'\hat{r}_l\right\rangle = 0, \tag{A23}$$

where the identity (A23) only exists for odd order correlation tensors.

A3.1 Kinematic relations for incompressible flow

Using the identity in Eqs. (A2) and (A21), $u_L = u_i\hat{r}_i$, and the product rule of differentiation,

$$\begin{aligned}&Q_{ijk,k}\hat{r}_i\hat{r}_j = \left\langle u_i u_j u_k'\hat{r}_i\hat{r}_j\right\rangle_{,k} - \left\langle u_i u_j u_k'\right\rangle\left(\hat{r}_i\hat{r}_j\right)_{,k}\\&= \left\langle u_L^2 u_k'\right\rangle_{,k} - \frac{1}{r}\left\langle u_i u_j u_k'\right\rangle\left(\hat{r}_j\delta_{ik} + \hat{r}_i\delta_{jk} - 2\hat{r}_i\hat{r}_j\hat{r}_k\right).\end{aligned} \tag{A24}$$

Using Eqs. (A6) and (A21), and the product rule of differentiation,

$$\begin{aligned}&Q_{ijk,k}\hat{r}_i\hat{r}_j = \left\langle u_L^2 u_L'\hat{r}_k\right\rangle_{,k} - \frac{1}{r}\left(2\left\langle u_L u_i u_i'\right\rangle - 2\left\langle u_L^2 u_L'\right\rangle\right)\\&= \left\langle u_L^2 u_L'\right\rangle_{,k}\hat{r}_k + \frac{2}{r}\left\langle u_L^2 u_L'\right\rangle - \frac{1}{r}\left(2\left\langle u_L u_i u_i'\right\rangle - 2\left\langle u_L^2 u_L'\right\rangle\right)\end{aligned} \tag{A25}$$

For incompressible flow, $Q_{ijk,k} = 0$. Kinematic relations for third order correlation functions can be easily derived from Eq. (A25)

$$2R_3 = \frac{1}{r^3}\left(r^4 L_3\right)_{,r}, 4T_3 = \frac{1}{r}\left(r^2 L_3\right)_{,r},$$

and (A26)

$$\left(r^2 L_3\right)_{,r} = r\left(2R_3 - 2L_3\right),$$

which are the same as our original results in Eq. (26).

A3.2 Kinematic relations for constant divergence on small scale

Eq. (A25) is still valid for constant divergence flow such that

$$\begin{aligned}Q_{ijk,k}\hat{r}_i\hat{r}_j = \theta\left\langle u_L^2\right\rangle &= \left\langle u_L^2 u_L'\right\rangle_{,k}\hat{r}_k + \frac{2}{r}\left\langle u_L^2 u_L'\right\rangle\\&\quad - \frac{1}{r}\left(2\left\langle u_L u_i u_i'\right\rangle - 2\left\langle u_L^2 u_L'\right\rangle\right),\end{aligned} \tag{A27}$$

from which we should have an exact relation (same as Eq. (31))

$$R_3 + \frac{1}{2}\left\langle u_L^2\right\rangle\theta r = \frac{1}{2r^3}\left(r^4 L_3\right)_{,r}. \tag{A28}$$

On the other hand, from identity (A23), we have

$$\begin{aligned}Q_{ijk,k}\delta_{ij} = \theta\left\langle u^2\right\rangle &= \left\langle u_i u_i u_k'\right\rangle_{,k} = \left\langle u_i u_i u_L'\hat{r}_k\right\rangle_{,k}\\&= \left\langle u^2 u_L'\right\rangle_{,r} + \frac{2}{r}\left\langle u^2 u_L'\right\rangle.\end{aligned} \tag{A29}$$

With $R_{31} = \langle u^2 u_L'\rangle$, another exact relation (same as Eq. (33)) is

$$\left\langle u^2\right\rangle\theta = \frac{1}{r^2}\left(r^2 R_{31}\right)_{,r}. \tag{A30}$$

With $\langle u^2\rangle \approx 3\langle u_L^2\rangle$, the kinematic relation reads (same as Eq. (34))

$$R_3 + \frac{1}{6r}\left(r^2 R_{31}\right)_{,r} = \frac{1}{2r^3}\left(r^4 L_3\right)_{,r}. \tag{A31}$$

A3.3 Kinematic relations for irrotational flow on large scale

Like the derivation for second order correlations in Eq. (A15), the starting point is the expression,

$$\begin{aligned}Q_{ijk,l}\varepsilon_{mkl}\varepsilon_{min}\hat{r}_j\hat{r}_n &= Q_{ijk,l}\left(\delta_{ik}\delta_{nl} - \delta_{nk}\delta_{il}\right)\hat{r}_j\hat{r}_n\\&= Q_{ijk,l}\left(\hat{r}_l\delta_{ik} - \hat{r}_k\delta_{il}\right)\hat{r}_j.\end{aligned} \tag{A32}$$

where an identity for Levi-Civita symbol is used

$$\varepsilon_{mkl}\varepsilon_{min} = \delta_{ik}\delta_{nl} - \delta_{nk}\delta_{il}. \tag{A33}$$

The curl free condition leads to $Q_{ijk,l}\varepsilon_{mkl} = 0$. Using the product rule of differentiation,

$$\begin{aligned}Q_{ijk,l}\left(\hat{r}_l\delta_{ik} - \hat{r}_k\delta_{il}\right)\hat{r}_j &= \left\langle u_i u_j u_i'\right\rangle_{,l}\hat{r}_j\hat{r}_l - \left\langle u_i u_j u_k'\right\rangle_{,i}\hat{r}_j\hat{r}_k\\&= \left\langle u_i u_j u_i'\hat{r}_j\right\rangle_{,l}\hat{r}_l - \left\langle u_i u_j u_i'\right\rangle\left(\hat{r}_j\right)_{,l}\hat{r}_l\\&\quad - \left\langle u_i u_j u_k'\hat{r}_j\hat{r}_k\right\rangle_{,i} + \left\langle u_i u_j u_k'\right\rangle\left(\hat{r}_j\hat{r}_k\right)_{,i} = 0.\end{aligned} \tag{A34}$$

Because $\langle u_i u_j u_i'\rangle(\hat{r}_j)_{,l}\hat{r}_l = \langle u_i u_j u_i'\rangle(\hat{r}_j)_{,r} = 0$ (from identity (A5)), Eq. (A34) becomes

$$\begin{aligned}&\left\langle u_L u_i u_i'\right\rangle_{,l}\hat{r}_l - \left\langle u_i u_L u_L'\right\rangle_{,i}\\&\qquad + \frac{1}{r}\left\langle u_i u_j u_k'\right\rangle\left(\hat{r}_j\delta_{ik} + \hat{r}_k\delta_{ij} - 2\hat{r}_i\hat{r}_j\hat{r}_k\right) = 0.\end{aligned} \tag{A35}$$

Again with identity in Eq. (A1), $u_L = u_i\hat{r}_i$, and the help of Eq. (A22),

$$\begin{aligned}&\left\langle u_L u_i u_i'\right\rangle_{,r} - \left\langle u_L^2 u_L'\hat{r}_i\right\rangle_{,i}\\&\qquad + \frac{1}{r}\left(\left\langle u_L u_i u_i'\right\rangle + \left\langle u_i u_i u_L'\right\rangle - 2\left\langle u_L^2 u_L'\right\rangle\right) = 0.\end{aligned} \tag{A36}$$

With production rule of differentiation for second term in Eq. (A36), we should have

$$R_{3,r} - \frac{2}{r}L_3 - L_{3,r} + \frac{1}{r}(R_3 + R_{31} - 2L_3) = 0. \tag{A37}$$

Finally, with $R_3 = L_3 + 2T_3$, kinematic relations are

$$\left(R_3 r\right)_{,r} + R_{31} = \frac{1}{r^3}\left(L_3 r^4\right)_{,r}, 3R_3 - R_{31} = \frac{2}{r^3}\left(r^4 T_3\right)_{,r},$$
and
$$3L_3 - R_{31} = 2\left(rT_3\right)_{,r}, \tag{A38}$$

which are the same as those developed before (Eq. (37)) but in a much more compact way.

A4 Formulating kinematic relations of arbitrary order

The new compact formulation for second and third order kinematic relations can be generalized to arbitrary order. Some tensor and vector algebra are involved, and readers can jump to main results. Equations (A57)-(A61) present the limiting values of correlation functions on small and large scales. General kinematic relations for different types of flow are also presented, i.e. Eqs. (A65)-(A68) for incompressible flow, Eqs. (A73)-(A77) for constant divergence flow on small scale, and Eqs. (A86)-(A88) for irrotational flow on large scale.

Just like in Sections A2 and A3, some general tensors and identities are introduced first. The pth order Ω tensor and its derivative reads

$${}_{(p)}\Omega_{ij\ldots kl} = \underbrace{(\hat{r}_i\hat{r}_j\ldots\hat{r}_k\hat{r}_l)}_{p}, \tag{A39}$$

$$\left({}_{(p)}\Omega_{ij\ldots kl}\right)_{,m} = \frac{\partial\left({}_{(p)}\Omega_{ij\ldots kl}\right)}{\partial r_m} = \frac{1}{r}\left({}_{(p+1)}\Pi_{ij\ldots klm} - p\left({}_{(p+1)}\Omega_{ij\ldots klm}\right)\right), \tag{A40}$$

where the Π tensor is written as

$${}_{(p+1)}\Pi_{ij\ldots klm} = \sum_{a,b..,d,e\in[S_p]^{p-1}} \hat{r}_a\hat{r}_b\ldots\hat{r}_d\delta_{em}. \tag{A41}$$

Equation (A40) is a generalization of identities in Eqs. (A1)-(A4). Here $[S_p]^{p-1}$ includes all subsets of size (p-1) in set $[S_p] = \{i, j, \ldots k, l\}$ of size p. There is total of p subsets of size (p-1) from set S_p of size p. Indices $a, b, ..d, e$ represent all possible combinations of size (p-1) from set S_p of size p. Here the Kronecker delta $\delta_{\bullet m}$ in Π tensor should always have m as one of its indices. There will be p terms for tensor ${}_{(p+1)}\Pi_{ij\ldots klm}$ of order (p+1).

One example of 4^{th} order Ω tensor is:

$$\left({}_{(4)}\Omega_{ijkl}\right)_{,m} = \left(\hat{r}_i\hat{r}_j\hat{r}_k\hat{r}_l\right)_{,m} = \frac{1}{r}\left({}_{(5)}\Pi_{ijklm} - 4\left({}_{(5)}\Omega_{ijklm}\right)\right), \tag{A42}$$

where 5^{th} order tensor Π is

$${}_{(5)}\Pi_{ijklm} = \hat{r}_i\hat{r}_j\hat{r}_l\delta_{km} + \hat{r}_i\hat{r}_k\hat{r}_l\delta_{jm} + \hat{r}_i\hat{r}_j\hat{r}_k\delta_{lm} + \hat{r}_j\hat{r}_k\hat{r}_l\delta_{im}. \tag{A43}$$

For odd number p, two additional tensors Λ and Σ of (p-1) order can be introduced consisting of Kronecker delta,

$${}_{(p-1)}\Lambda_{ijkl\ldots mn} = \delta_{ij}\delta_{kl}\ldots\delta_{mn} \quad \text{with} \quad (p-1)/2 \quad \text{terms in multiplication}, \tag{A44}$$

$${}_{(p-1)}\Sigma_{ijkl\ldots mn} = \delta_{ij}\delta_{kl}\ldots + \delta_{ik}\delta_{jl}\ldots + \ldots \quad \text{with} \quad \frac{(p-1)!}{2^{(p-1)/2}\left((p-1)/2\right)!} \quad \text{terms in summation}. \tag{A45}$$

Examples of 4^{th} order Λ and Σ tensors are:

$${}_{(4)}\Lambda_{ijkl} = \delta_{ij}\delta_{kl} \quad \text{and} \quad {}_{(4)}\Sigma_{ijkl} = \delta_{ij}\delta_{kl} + \delta_{ik}\delta_{jl} + \delta_{il}\delta_{jk}. \tag{A46}$$

With the help of Eq. (A40), two additional identities can be established for tensor Ω,

$$\left({}_{(p)}\Omega_{ij\ldots kl}\right)_{,r} = \left({}_{(p)}\Omega_{ij\ldots kl}\right)_{,m}\hat{r}_m = \left(\hat{r}_i\hat{r}_j\ldots\hat{r}_k\hat{r}_l\right)_{,m}\hat{r}_m = 0, \tag{A47}$$

$$\left({}_{(p)}\Omega_{ij\ldots kl}\right)_{,l} = \left({}_{(p)}\Omega_{ij\ldots kl}\right)_{,m}\delta_{lm} = \frac{2}{r}\left({}_{(p-1)}\Omega_{ij\ldots k}\right). \tag{A48}$$

A4.1 Correlation functions and identities for any type of flow

The two-point velocity correlation tensor Q of arbitrary order p can be defined as,

$$\left({}_{(p)}Q_{ijk..mn}\right) = \left\langle u_i u_j u_k \ldots u_m u_n^{'}\right\rangle. \tag{A49}$$

Two identities for Q tensor of any order p are (similar to Eq. (A21)),

$$\left\langle u_i u_j u_k \ldots u_m \ldots u_n^{'}\right\rangle \underbrace{\delta_{ij}\delta_{\ldots}\ldots}_{q}\underbrace{(\hat{r}_k\ldots\hat{r}_m)}_{p-q-1}(\delta_{ns} - \hat{r}_n\hat{r}_s) = \left\langle u^q u_L^{p-q-1}u_n^{'}\right\rangle(\delta_{ns} - \hat{r}_n\hat{r}_s) = \left\langle u^q u_L^{p-q-1}u_s^{'}\right\rangle - \left\langle u^q u_L^{p-q-1}u_L^{'}\hat{r}_s\right\rangle = 0, \tag{A50}$$

and

$$\left\langle u_i u_j u_k \ldots u_m \ldots u_n^{'}\right\rangle \underbrace{\delta_{jk}\delta_{\ldots}\ldots}_{q}\underbrace{(\hat{r}_m\ldots\hat{r}_n)}_{p-q-1}(\delta_{is} - \hat{r}_i\hat{r}_s) = \left\langle u^q u_L^{p-q-2}u_i u_L^{'}\right\rangle(\delta_{is} - \hat{r}_i\hat{r}_s) = \left\langle u^q u_L^{p-q-2}u_s u_L^{'}\right\rangle - \left\langle u^q u_L^{p-q-1}u_L^{'}\hat{r}_s\right\rangle = 0, \tag{A51}$$

where q is an even number that stands for q indices in term $(\delta_{ij}\delta_{\ldots}\ldots)$. Scalar correlation functions are defined by tensor contraction of Q.

For even number q, the total correlation functions of order $(p, q{+}1)$ is defined as

$$R_{(p,q+1)} = \left\langle u^q u_L^{p-q-2}u_i u_i^{'}\right\rangle = \left\langle u^q u_L^{p-q-2}\mathbf{u}\cdot\mathbf{u}^{'}\right\rangle. \tag{A52}$$

For even number q, the longitudinal and transverse correlation functions of order (p, q) are

$$L_{(p,q)} = \left\langle u^q u_L^{p-q-1}u_L^{'}\right\rangle \tag{A53}$$

and

$$T_{(p,q)} = \left(R_{(p,q+1)} - L_{(p,q)}\right)/2. \tag{A54}$$

Figure 2 lists the velocity correlation functions up to the sixth order. Just like the second order correlations, all these correlation functions can be similarly computed from N-body simulations.

A4.2 Correlation functions in the limit $r \to 0$ and $r \to \infty$

In the limit $r \to 0$ on small scale, the r dependence is eliminated and isotropic homogeneous velocity correlation tensor $\mathbf{Q}$ of odd order p should satisfy (see Eq. (11) as an example):

$$\lim_{r\to 0}\left({}_{(p)}Q_{ij..klm}\right)_{,m} = C_p \cdot {}_{(p-1)}\sum_{ij..kl}, \tag{A55}$$

such that with the definition of Σ tensor in Eq. (A45), we have

$$\lim_{r\to 0}\left\langle u^q u_L^{p-q-1}\right\rangle\theta = \lim_{r\to 0}\left({}_{(p)}Q_{ijk..lm}\right)_{,m}\underbrace{\delta_{ij}\delta_{..}..}_{q}\underbrace{(\hat{r}_k...\hat{r}_l)}_{p-q-1}$$
$$= C_p\frac{p!}{2^{(p-1)/2}\left((p-1)/2\right)!\,(p-q)}. \tag{A56}$$

where C_p is a parameter that is only dependent on the order p. Here $\theta = u_{i,i}$ is the divergence on small scale.

The limiting ratio for odd order p reads

$$\lim_{r\to 0}\frac{\left\langle u^q u_L^{p-q-1}\right\rangle}{\left\langle u_L^{p-1}\right\rangle} = \frac{p}{p-q} \quad \text{with q=0...p-1}. \tag{A57}$$

Equation (A57) is also valid for $r \to \infty$where velocity distributions are independent of scale r, i.e.

$$\lim_{r\to\infty}\frac{\left\langle u^q u_L^{p-q-1}\right\rangle}{\left\langle u_L^{p-1}\right\rangle} = \frac{p}{p-q} \quad \text{with q=0...p-1}. \tag{A58}$$

Finally, using the definition of correlation functions from index contraction, for correlation functions of odd order p,

$$\lim_{r\to 0,\infty}\frac{L_{(p,q)}}{L_{(p,0)}} = \lim_{r\to 0,\infty}\frac{\left\langle u^q u_L^{p-q-1}\right\rangle}{\left\langle u_L^{p-1}\right\rangle} = \frac{p}{p-q}. \tag{A59}$$

Similar relations can be obtained for correlation functions of even order p (from Eq. (A58)),

$$\lim_{r\to 0}\frac{R_{(p,q+1)}}{L_{(p,0)}} = \lim_{r\to 0}\frac{\left\langle u^q u_L^{p-q-2}\mathbf{u}\cdot\mathbf{u}'\right\rangle}{\left\langle u_L^{p-1}u_L'\right\rangle} = \frac{p+1}{p-q-1}, \tag{A60}$$

and

$$\lim_{r\to 0,\infty}\frac{L_{(p,q)}}{L_{(p,0)}} = \lim_{r\to 0,\infty}\frac{\left\langle u^q u_L^{p-q-1}u_L'\right\rangle}{\left\langle u_L^{p-1}u_L'\right\rangle} = \frac{p+1}{p+1-q}. \tag{A61}$$

A4.3 Kinematic relations for incompressible flow

The incompressibility condition requires a vanishing divergence of correlation tensor Q

$$\left({}_{(p)}Q_{ij..mn}\right)_{,n} = \left\langle u_i u_j ... u_m u_n'\right\rangle_{,n} = 0. \tag{A62}$$

Using Eq. (A62), the relation $u_L = u_i\hat{r}_i$, and the product rule of differentiation,

$$\left\langle u_i u_j u_k ... u_m u_n'\right\rangle_{,n}\underbrace{\delta_{ij}\delta_{..}..}_{q}\underbrace{(\hat{r}_k...\hat{r}_m)}_{p-q-1}$$
$$= \left[\left\langle u_i u_j u_k ... u_m u_n'\right\rangle\delta_{ij}...(\hat{r}_k...\hat{r}_m)\right]_{,n}$$
$$- \left\langle u_i u_j u_k ... u_m u_n'\right\rangle\delta_{ij}...(\hat{r}_k...\hat{r}_m)_{,n} = 0, \tag{A63}$$

where q is an even number that stands for q indices in term $(\delta_{ij}\delta_{..}...)$. Using identities (A50) and (A40), Eq. (A63) becomes

$$\left\langle u^q u_L^{p-q-1}u_L'\hat{r}_n\right\rangle_{,n} = \left\langle u^q u_k ... u_m u_n'\right\rangle(\hat{r}_k...\hat{r}_m)_{,n}$$
$$= \left\langle u^q u_k ... u_m u_n'\right\rangle\frac{1}{r}\left[{}_{(p-q)}\Pi_{k...mn} - (p-q-1)(\hat{r}_k...\hat{r}_m\hat{r}_n)\right]. \tag{A64}$$

Applying the product rule of differentiation on the left side of Eq. (A64) and the definition of velocity correlation functions in Eqs. (A52), (A54) and tensor Π in Eq. (A41), we have

$$\left(L_{(p,q)}\right)_{,r} + \frac{2}{r}L_{(p,q)} = \frac{1}{r}(p-q-1)\left(R_{(p,q+1)} - L_{(p,q)}\right) \tag{A65}$$

Finally, kinematic relations for correlation functions of arbitrary order p should be

$$(p-q-1)R_{(p,q+1)} = \frac{1}{r^{p-q}}\left(r^{p-q+1}L_{(p,q)}\right)_{,r}, \tag{A66}$$

$$2(p-q-1)T_{(p,q)} = \frac{1}{r}\left(r^2 L_{(p,q)}\right)_{,r}, \tag{A67}$$

$$\left(r^2 R_{(p,q+1)}\right)_{,r} = \frac{2}{r^{p-q-1}}\left(r^{p-q+1}T_{(p,q)}\right)_{,r}. \tag{A68}$$

A4.4 Kinematic relations for constant divergence on small scale

Just like the incompressible flow, we start from the equation

$$\left\langle u^q u_L^{p-q-1}\right\rangle\theta = \left\langle u_i u_j u_k ... u_m u_n'\right\rangle_{,n}\underbrace{\delta_{ij}\delta_{..}..}_{q}\underbrace{(\hat{r}_k...\hat{r}_m)}_{p-q-1}$$
$$= \left[\left\langle u_i u_j u_k ... u_m u_n'\right\rangle\delta_{ij}\delta_{..}..(\hat{r}_k...\hat{r}_m)\right]_{,n}$$
$$- \left\langle u_i u_j u_k ... u_m u_n'\right\rangle\delta_{ij}\delta_{..}..(\hat{r}_k...\hat{r}_m)_{,n}, \tag{A69}$$

where q is an even number. Using identities (A50) and (A40), Eq. (A69) becomes

$$\left\langle u^q u_L^{p-q-1}\right\rangle\theta = \left\langle u^q u_L^{p-q-1}u_n'\right\rangle_{,n}$$
$$- \left\langle u^q u_k ... u_m u_n'\right\rangle\frac{1}{r}\left[{}_{(p-q)}\Pi_{k...mn} - (p-q-1)(\hat{r}_k...\hat{r}_m\hat{r}_n)\right]. \tag{A70}$$

Applying the product rule of differentiation to the first item on the RHS and the definition of correlation functions in Eqs. (A52) and (A54), a general relation for constant divergence flow is

$$(p-q-1)R_{(p,q+1)} + \left\langle u^q u_L^{p-q-1}\right\rangle\theta r$$
$$= \frac{1}{r^{p-q}}\left(r^{p-q+1}L_{(p,q)}\right)_{,r}. \tag{A71}$$

Equation (A71) is a general relation for correlation functions of any order p. For correlation functions of even order p (Note that q is always an even number),

$$\lim_{r\to 0}\left\langle u^q u_L^{p-q-1}\right\rangle = 0. \tag{A72}$$

Therefore, the kinematic relations for even order correlations in constant divergence flow should be the same as that of incompressible flow, i.e. using Eqs. (A71) and (A72), Eqs. (A66)-(A68) are still valid for correlation functions of even order p in constant divergence flow.

For odd order p, two special cases are considered with $q = p-1$ and $q = 0$ from Eq. (A71),

$$\left\langle u^{p-1}\right\rangle \theta r = \frac{1}{r}\left(r^2 L_{(p,p-1)}\right)_{,r} \tag{A73}$$

and

$$(p-1)\, R_{(p,1)} + \left\langle u_L^{p-1}\right\rangle \theta r = \frac{1}{r^p}\left(r^{p+1} L_{(p,0)}\right)_{,r}. \tag{A74}$$

For $r \to 0$, the correlation function $L_{(p,p-1)}$ can be solved from Eq. (A73) (use Eq. (A57))

$$L_{(p,p-1)} = \frac{p}{3}\theta\left\langle u_L^{p-1}\right\rangle r = \frac{1}{3}\theta\left\langle u^{p-1}\right\rangle r. \tag{A75}$$

For $p = 1$ and $q = 0$ in Eq. (A74), the mean pairwise velocity $S_1^{lp}(r) = \langle \Delta u_L\rangle = \left\langle u_L^{'} - u_L\right\rangle = 2\left\langle u_L^{'}\right\rangle$ can be directly related to the divergence,

$$\theta = \frac{1}{2r^2}\left(r^2\langle \Delta u_L\rangle\right)_{,r}. \tag{A76}$$

With $\langle \Delta u_L\rangle = -Har$ from stable clustering hypothesis, the divergence $\theta = -3Ha/2$ on small scale. Equation (A76) is derived for constant divergence flow. With Eq. (A57), Eqs. (A71) and (A74), the kinematic relations for odd order p should read

$$\begin{aligned}(p-q-1)\, R_{(p,q+1)} + \frac{1}{p-q}\frac{1}{r}\left(r^2 L_{(p,p-1)}\right)_{,r} \\ = \frac{1}{r^{p-q}}\left(r^{p-q+1} L_{(p,q)}\right)_{,r}.\end{aligned} \tag{A77}$$

A4.5 Kinematic relations for irrotational flow on large scale

The irrotational flow requires a vanishing curl, i.e. $Q_{ij\ldots kl,m}\varepsilon_{nlm} = 0$, such that

$$\begin{aligned}&\left\langle u_i u_j \ldots u_k u_o u_l^{'}\right\rangle_{,m} \varepsilon_{nlm}\varepsilon_{nis} \underbrace{\delta_{jk}\delta_{\ldots}}_{q} \underbrace{(\ldots\hat{r}_o\hat{r}_s)}_{p-q-1} \\ &= \left\langle u_i u_j \ldots u_k u_o u_l^{'}\right\rangle_{,m} (\delta_{il}\delta_{ms} - \delta_{im}\delta_{ls}) \underbrace{\delta_{jk}\delta_{\ldots}}_{q} \underbrace{(\ldots\hat{r}_o\hat{r}_s)}_{p-q-1} = 0.\end{aligned} \tag{A78}$$

where the identity $\varepsilon_{nlm}\varepsilon_{nis} = (\delta_{il}\delta_{ms} - \delta_{im}\delta_{ls})$ is used and q is an even number for q indices in term $\delta_{ij}\delta_{\ldots}\ldots$ From Eq. (A78),

$$\begin{aligned}&\left\langle u_i u_j \ldots u_k u_o u_l^{'}\right\rangle_{,m} (\delta_{il}\hat{r}_m) \underbrace{\delta_{jk}\delta_{\ldots}}_{q} \underbrace{(\ldots\hat{r}_o)}_{p-q-2} \\ &= \left\langle u_i u_j \ldots u_k u_o u_l^{'}\right\rangle_{,m} (\delta_{im}\hat{r}_l) \underbrace{\delta_{jk}\delta_{\ldots}}_{q} \underbrace{(\ldots\hat{r}_o)}_{p-q-2} \\ &= \left\langle u_i u_j \ldots u_k u_o u_l^{'}\right\rangle_{,i} \underbrace{\delta_{jk}\delta_{\ldots}}_{q} \underbrace{(\ldots\hat{r}_o\hat{r}_l)}_{p-q-1}.\end{aligned} \tag{A79}$$

Using the product rule of differentiation, the LHS (left hand side) in Eq. (A79) becomes

$$\begin{aligned}LHS &= \left(\left({}_{(p)}Q_{ij\ldots kl}\right)\delta_{il}\left({}_{(p-2)}\Omega_{j\ldots k}\right)\right)_{,m}\hat{r}_m \\ &- \left({}_{(p)}Q_{ij\ldots kl}\right)\delta_{il}\left({}_{(p-2)}\Omega_{j\ldots k}\right)_{,m}\hat{r}_m\end{aligned}$$

or equivalently

$$LHS = \left\langle u^q u_L^{p-q-2}\mathbf{u}\cdot\mathbf{u}^{'}\right\rangle_{,m}\hat{r}_m - \left\langle u^q \ldots u_o \mathbf{u}\cdot\mathbf{u}^{'}\right\rangle(\ldots\hat{r}_o)_{,m}\hat{r}_m. \tag{A80}$$

Using identity (A47), $(\ldots\hat{r}_o)_{,m}(\hat{r}_m) = 0$, LHS term becomes

$$\begin{aligned}LHS &= \left\langle u^q u_L^{p-q-2}\mathbf{u}\cdot\mathbf{u}^{'}\right\rangle_{,m}(\hat{r}_m) \\ &= \left\langle u^q u_L^{p-q-2}\mathbf{u}\cdot\mathbf{u}^{'}\right\rangle_{,r} = \left(R_{p,q+1}\right)_{,r}.\end{aligned} \tag{A81}$$

Now, using the product rule of differentiation, the right-hand side (RHS) in Eq. (A79) reads,

$$RHS = \left\langle u^q u_L^{p-q-2} u_i u_L^{'}\right\rangle_{,i} - \left\langle u^q u_i \ldots u_o u_l^{'}\right\rangle(\ldots\hat{r}_o\hat{r}_l)_{,i}. \tag{A82}$$

Using identity (A40), the right-hand-side term becomes

$$\begin{aligned}RHS &= \left\langle u^q u_L^{p-q-2} u_i u_L^{'}\right\rangle_{,i} \\ &- \frac{1}{r}\left\langle u^q u_i \ldots u_o u_l^{'}\right\rangle\left[{}_{(p-q)}\Pi_{\ldots oli} - (p-q-1)(\ldots\hat{r}_o\hat{r}_l\hat{r}_i)\right].\end{aligned} \tag{A83}$$

Using identity (A51), definition in (A41), (A52), and (A54),

$$\begin{aligned}RHS &= \left\langle u^q u_L^{p-q-1} u_L^{'}\hat{r}_i\right\rangle_{,i} - \frac{1}{r}\left(\left\langle u^q u_L^{p-q-2}\mathbf{u}\cdot\mathbf{u}^{'}\right\rangle\right. \\ &\left. + (p-q-2)\left\langle u^{q+2} u_L^{p-q-3} u_L^{'}\right\rangle - (p-q-1)\left\langle u^q u_L^{p-q-1} u_L^{'}\right\rangle\right).\end{aligned} \tag{A84}$$

Again, applying the product rule of differentiation on the first term of RHS of Eq. (A84) leads to,

$$\begin{aligned}RHS &= L_{(p,q)} + \frac{2}{r}L_{(p,q)} - \frac{1}{r}\left(R_{(p,q+1)}\right. \\ &\left. + (p-q-2)\, L_{(p,q+2)} - (p-q-1)\, L_{(p,q)}\right).\end{aligned} \tag{A85}$$

Equating Eq. (A85) with Eq. (A81) leads to the final kinematic relations between velocity correlation functions of arbitrary order p and even number $0 \leqslant q \leqslant p-1$,

$$\begin{aligned}\left(R_{(p,q+1)} r\right)_{,r} + (p-q-2)L_{(p,q+2)} \\ = \frac{1}{r^{p-q}}\left(r^{p-q+1} L_{(p,q)}\right)_{,r},\end{aligned} \tag{A86}$$

$$\begin{aligned}(p-q)\, R_{(p,q+1)} - (p-q-2)L_{(p,q+2)} \\ = \frac{2}{r^{p-q}}\left(r^{p-q+1} T_{(p,q)}\right)_{,r},\end{aligned} \tag{A87}$$

$$(p-q)\, L_{(p,q)} - (p-q-2)\, L_{(p,q+2)} = 2\left(rT_{(p,q)}\right)_{,r}. \tag{A88}$$

In Eqs. (A86)-(A88), terms involving correlation function $L_{(p,q+2)}$ should vanish if $q \geqslant p-2$.